SDSS unveils a population of intrinsically faint cataclysmic variables at the minimum orbital period

B. T. Gänsicke,[1]⋆ M. Dillon,[1] J. Southworth,[1] J. R. Thorstensen,[2] P. Rodríguez-Gil,[3,4]
A. Aungwerojwit,[1,5] T. R. Marsh,[1] P. Szkody,[6] S. C. C. Barros,[1] J. Casares,[4]
D. de Martino,[7] P. J. Groot,[8] P. Hakala,[9] U. Kolb,[10] S. P. Littlefair,[11]
I. G. Martínez-Pais,[4,12] G. Nelemans[8] and M. R. Schreiber[13]

[1]*Department of Physics, University of Warwick, Coventry CV4 7AL*
[2]*Department of Physics and Astronomy, Dartmouth College, 6127 Wilder Laboratory, Hanover, NH 03755-3528, USA*
[3]*Isaac Newton Group of Telescopes, Apartado de correos 321, E-38700 Santa Cruz de la Palma, Tenerife, Spain*
[4]*Instituto de Astrofísica de Canarias, 38200 La Laguna, Tenerife, Spain*
[5]*Department of Physics, Faculty of Science, Naresuan University, Phitsanulok, 65000, Thailand*
[6]*Astronomy Department, University of Washington, Seattle, WA 98195, USA*
[7]*INAF - Osservatorio di Capodimonte, Via Moiariello 16, 80131 Napoli, Italy*
[8]*Department of Astrophysics, IMAPP, Radboud University Nijmegen, PO Box 9010, 6500 GL Nijmegen, the Netherlands*
[9]*Tuorla Observatory, University of Turku, Vaisalantie 20, FIN-21500 Piikkio, Finland*
[10]*Department of Physics and Astronomy, The Open University, Walton Hall, Milton Keynes MK7 6AA*
[11]*Department of Physics and Astronomy, University of Sheffield, Sheffield, S3 7RH*
[12]*Departamento de Astrofísica, Universidad de La Laguna, E-38206 La Laguna, Tenerife, Spain*
[13]*Departamento de Física y Astronomía, Facultad de Ciencias, Universidad de Valparaíso, Valparaíso, Chile*

ABSTRACT

We discuss the properties of 137 cataclysmic variables (CVs) which are included in the Sloan Digital Sky Survey (SDSS) spectroscopic data base, and for which accurate orbital periods have been measured. 92 of these systems are new discoveries from SDSS and were followed-up in more detail over the past few years. 45 systems were previously identified as CVs because of the detection of optical outbursts and/or X-ray emission, and subsequently re-identified from the SDSS spectroscopy. The period distribution of the SDSS CVs differs dramatically from that of all the previously known CVs, in particular it contains a significant accumulation of systems in the orbital period range 80–86 min. We identify this feature as the elusive 'period minimum spike' predicted by CV population models, which resolves a long-standing discrepancy between compact binary evolution theory and observations. We show that this spike is almost entirely due to the large number of CVs with very low accretion activity identified by SDSS. The optical spectra of these systems are dominated by emission from the white dwarf photosphere, and display little or no spectroscopic signature from the donor stars, suggesting very low mass companion stars. We determine the average absolute magnitude of these low-luminosity CVs at the period minimum to be $\langle M_g \rangle = 11.6 \pm 0.7$. Comparison of the SDSS CV sample to the CVs found in the Hamburg Quasar Survey and the Palomar Green Survey suggests that the depth of SDSS is the key ingredient resulting in the discovery of a large number of intrinsically faint short-period systems.

Key words: binaries: close – stars: dwarf novae – stars: evolution – novae, cataclysmic variables – stars: statistics.

1 INTRODUCTION

Compact binary stars (CBs) are central to a variety of astrophysical contexts such as short γ-ray bursts, which are thought to arise from neutron star mergers (Paczynski 1986; Berger et al. 2005; Gehrels et al. 2005); supernovae Type Ia, whose progenitors are white dwarf (WD) binaries (Whelan & Iben 1973; Woosley, Taam & Weaver 1986; Ruiz-Lapuente et al. 2004); or stellar black holes (Casares, Charles & Naylor 1992). Despite the fundamental importance of CBs on a wide range of astronomical scales, our understanding of their evolution is rather fragmentary. Major uncertainties lie in the

⋆E-mail: boris.gaensicke@warwick.ac.uk

common envelope phase, when the more massive of the two stars evolves into a red giant and engulfs the other one (e.g. Nelemans & Tout 2005), and in the subsequent orbital angular momentum losses such as magnetic stellar wind braking (Verbunt & Zwaan 1981; Kalogera, Kolb & King 1998; Justham, Rappaport & Podsiadlowski 2006).

Cataclysmic variables (CVs) are compact binaries containing a WD accreting from a Roche-lobe filling main sequence, slightly evolved, or brown dwarf donor and represent an abundant class of CBs that are well suited for observational tests of CB evolution theory. However, while detailed CV population models have been calculated (e.g. Kolb 1993; Politano 1996; Howell, Nelson & Rappaport 2001), and more than 600 CVs have been observed in some detail (Ritter & Kolb 2003), the disagreement between theory and observations has been a continuous source of frustration for the past two decades.

CVs with main sequence or slightly evolved donors evolve towards shorter orbital periods through the loss of angular momentum by magnetic braking (Verbunt & Zwaan 1981; Rappaport, Joss & Verbunt 1983) and gravitational radiation (Faulkner 1971; Paczynski & Sienkiewicz 1981) until the mass of the donor becomes too low to sustain hydrogen burning, and the donor starts to become degenerate. At this point, the orbital period evolution reverses sign so that the period increases with time, and hence a very strong prediction of CV evolution theory is the existence of a minimum orbital period (Rappaport, Joss & Webbink 1982; Paczyński & Sienkiewicz 1983). Early estimates predicted the period minimum to occur around $P_{min} \simeq 60$–80 min (Paczynski & Sienkiewicz 1981; Rappaport et al. 1982), whilst more recent work using improved physics in the modelling of low-mass stars results in $P_{min} \simeq 65$–70 min (Kolb & Baraffe 1999; Howell et al. 2001). While a sharp minimum is detected in the period distribution of the currently known CVs (e.g. Knigge 2006), it is found at $\simeq 76$ min. This value is significantly longer than the predicted value, which could imply additional sinks of angular momentum loss besides gravitational wave radiation (e.g. Patterson 1998), and/or problems in understanding the structure of mass-losing low-mass stars.

Since the detection probability of a system at a given range in orbital period (P_{orb}) is proportional to the time it requires to evolve through that range, $N(P_{orb}) \propto 1/|\dot{P}_{orb}|$, a significant accumulation of CVs at the minimum period is expected. This accumulation is often dubbed *the period minimum spike* (Kolb & Baraffe 1999). Confronting theory and observations, it is clear that such a spike is absent in the period distribution of the known CVs (Patterson 1998; Gänsicke, Hagen & Engels 2002; Knigge 2006). This absence of the predicted pile-up of systems near the minimum period among the observed CVs has been one of the most intensively debated discrepancies between CV evolution theory and observations (Patterson 1998; Kolb & Baraffe 1999; King, Schenker & Hameury 2002; Barker & Kolb 2003; Willems et al. 2005), casting doubts on our understanding of compact binary evolution in general.

A major uncertainty on the observational side has been the fact that the known sample of CVs is a rather mixed bag of systems discovered by a variety of methods, such as variability, X-ray emission or blue colour. It is therefore subject to complex selection effects (Gänsicke 2005), and should not be expected to provide a genuine representation of the intrinsic properties of the Galactic CV population. In particular, all conventional CV discovery methods favour systems with intermediate mass transfer rates,[1] i.e. systems that are characterized by frequent outbursts or large X-ray luminosities. Consequently, the observed sample of CVs is likely to under-represent systems with low mass transfer rates, as they rarely undergo outbursts and are X-ray faint. Those are, however, exactly the properties predicted by population models for old, short-period systems, which are thought to make up the majority of all CVs (Kolb 1993; Howell, Rappaport & Politano 1997).

The CV sample identified in the Sloan Digital Sky Survey (SDSS) (Szkody et al. 2002c, 2003a, 2004, 2005, 2006, 2007a, 2009) has the potential to overcome many of the limitations of existing samples, as it extends to fainter objects and covers a wider range in colour space than any previous optical survey. In a series of earlier papers, we have explored the properties of individual SDSS CVs (e.g. Szkody et al. 2003b; Wolfe et al. 2003; Peters & Thorstensen 2005; Gänsicke et al. 2006; Littlefair et al. 2006a; Southworth et al. 2006, 2007b; Dillon et al. 2008). Here, we compile accurate orbital period measurements for 137 SDSS CVs, and show that the period distribution of these systems differs dramatically from all previously examined samples. In particular, a clear accumulation of systems in the period range 80–86 min is observed, consistent with the prediction of a period minimum spike made by the population models. Furthermore, we show that the bulk of the systems in this spike display distinctly different properties from the average short-period ($\lesssim 120$ min) CV.

2 ACCURATE ORBITAL PERIOD MEASUREMENTS OF SDSS CATACLYSMIC VARIABLES

For the purpose of quantitative comparison between the orbital period distribution of an observed sample of CVs and that of a population model, care has to be taken over the period measurements included in the observed distribution. For the convenience of the reader unfamiliar with the observational techniques, we briefly outline the caveats of CV orbital period determinations before describing the details of our compilation of accurate SDSS CV period measurements.

Orbital period determinations of CVs are generally achieved by one of two methods: time-resolved spectroscopy probing for radial velocity variations of at least one component in the CV, and time-resolved photometry probing for coherent variability of the system's brightness. Both methods can yield straightforward and unambiguous results, e.g. using the radial velocities measured from sharp absorption lines associated with the donor star, or from the detection of eclipses in the light curve. However, in a large fraction of CVs, more care has to be taken in the interpretation of the observations, as e.g. radial velocities measured from emission lines in low-resolution spectroscopy may reflect the unresolved motion

---

[1] Ironically, non-magnetic CVs with high mass transfer rates are also missed by the main identification methods, i.e. the detection of large-amplitude variability or X-ray emission. The reason for this is that these systems contain accretion discs in a hot, stable state with no occurrence of outbursts, and little X-ray emission from the boundary layer on the WD. A substantial number of bright high mass transfer systems has only been found in blue colour and/or emission line surveys, such as the Palomar Green (PG) Survey (e.g. Thorstensen, Davis & Ringwald 1991) or the Hamburg Quasar Survey (HQS; Aungwerojwit et al. 2005; Rodríguez-Gil et al. 2007b). A recent example for previously mis-identified bright CVs is the 11th magnitude system LS IV-08°3, which was thought to be an OB star, but is in fact a nova-like variable (Stark et al. 2008).

of different components within the CV, or red-noise and flickering in light curves may mimic a periodic brightness modulation. Such systematic problems can often, but not always, be overcome by increasing the spectral and/or temporal resolution, signal-to-noise ratio and the total quantity of data accumulated for a given system. Given the typical oversubscription on telescopes, it is an unfortunate fact that observers have to strike a difficult balance between the number of systems that can be followed up and the quality of parameters determined for each of them.

Even if the nature of the variability used to determine the orbital period is unambiguous, the details of the temporal sampling of the observations have a crucial impact on the quality of the orbital period measurement that can be obtained from the observational data. In particular, the accuracy of the period measurement is limited by the length of the observations. Except for coordinated multilongitude observations, the immediate limit on this is set by the seasonal visibility of a given object, which will in the best case be equal to the length of the observing night. Given that CV periods are in the range from 80 min to about a day, a single night of data will hence cover at most a few orbital cycles, and the typical lower limit on the error of orbital periods from such data is ~10 per cent. More accurate period determinations are obtained by combining data obtained over a number of nights. However, this potential for an improved period measurement comes at the price of an additional uncertainty. As the CV orbital periods are often much shorter than a day, the number of orbital cycles in between the two, or more, observing nights may be ambiguous, which is known as cycle-count uncertainty, or aliasing. Thorstensen & Freed (1985) discuss in detail Monte Carlo techniques that allow the probability of different cycle-count aliases to be established. A different approach using bootstrapping is given by Southworth et al. (2006).

Our aim in this paper is to establish the detailed orbital period distribution of the SDSS CVs,[2] which represent the largest CV sample selected in a homogenous way. For this purpose, we inspected the published orbital period measurements of every individual SDSS CV according to the caveats mentioned above, and excluded systems where the relative error on the orbital period measurement exceeded 3 per cent, or where we had substantial doubt about the correct choice of the cycle count alias.

In addition to direct orbital period measurements, we also considered indirect orbital period estimates for CVs exhibiting photometric variability in the form of superhumps, which are thought to be related to tidal interactions between the donor star and the accretion disc. Stolz & Schoembs (1984) published an empirical relation between the superhump period (P_{sh}) and the orbital period, which has been updated on several occasions throughout the years. We decided to investigate the method once more. Patterson et al. (2005) provide a recent compilation of CVs with reliable orbital and superhump periods. While there is a clear correlation of the superhump excess $\epsilon = (P_{sh} - P_{orb})/P_{orb}$ and the orbital period, a few clear outliers are present at short orbital periods and small values of ϵ, most of which are 'WZ Sge' systems (CVs with very long intervals between dwarf nova outbursts and extreme mass ratios). We restricted the following analysis to CVs below the period

---

[2] We exclude from our analysis the AM CVn stars, which are ultrashort-period helium-rich double-degenerate binaries that are not included in the standard CV population models. We also exclude SDSS J102347.68+003841.1 (FIRST J1023.6+003841; Bond et al. 2002; Thorstensen & Armstrong 2005; Homer et al. 2006a), which has recently been confirmed as a neutron star binary.
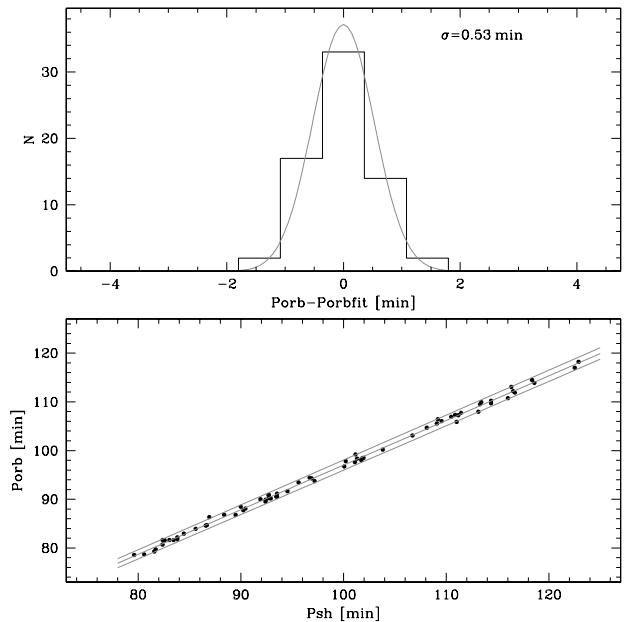

Figure 1. The $P_{sh}-P_{orb}$ relation. Bottom panel: 68 systems from Patterson et al. (2005) with $P_{orb} < 120$ min, i.e. below the period gap. Shown as grey lines are the best linear fit and its 1σ errors. Top panel: the histogram shows the distribution of observed minus computed (equation 1) orbital periods. The distribution is well fit by a Gaussian with a standard deviation of 0.53 min.

gap, where the bulk of the well-studied (and well-behaved) systems lie, and where the majority of the application of this method will take place. This leaves 68 CVs from the list of Patterson et al. (2005) (Fig. 1, bottom panel). We then fitted a linear relation to the (P_{sh}, P_{orb}) data,

$$P_{orb} = 0.9162(52)P_{sh} + 5.39(52), \qquad (1)$$

where both periods are given in minutes. In order to assess the error of orbital periods estimated in this way, we calculated for all 68 systems P_{orb} values from equation (1) and computed the differences from their actual orbital periods. The observed minus calculated P_{orb}s follow approximately a Gaussian distribution with a standard deviation of 0.53 min (Fig. 1, top panel). We conclude that accurate estimates of orbital periods can be obtained from reliable superhump periods. In the context of this paper, we assume a somewhat more pessimistic error on the superhump-based orbital periods of 2 min, which accounts for the small drifts in P_{sh} often observed during the evolution of the dwarf nova outburst. The orbital periods obtained from superhumps included in our analysis below range from 89.6 (SDSS J1653+2010) to 150 min (SDSS J1627+1204), with the latter one being the only system for which we extrapolated equation (1) above the range used for the calibration of the method.

The SDSS CVs that passed our scrutiny are listed in Table 1 for CVs that were identified from SDSS spectroscopy, and in Table 2 for those CVs which were previously known, and re-identified as CVs from the SDSS spectra.

3 THE ORBITAL PERIOD DISTRIBUTION OF THE SDSS CATACLYSMIC VARIABLES

The fibre allocation of SDSS does not cross-correlate with astronomical catalogues such as Simbad, and hence the nature of targets for spectroscopic follow-up may be known prior to the SDSS observation. For the following discussion, we shall call SDSS CVs all

Table 1. CVs identified by SDSS (new SDSS CVs) with reliable orbital period determinations. Orbital periods followed by '∗' are calculated from equation (1), but assuming a somewhat more pessimistic error of 2 min. The *g* magnitude refers to the typical state of the system, i.e. quiescence for dwarf novae and high state for nova-like variables. The CV subtype is given as DN = dwarf nova, i.e. at least one optical outburst has been detected; AM = AM Her star, i.e. the system shows characteristics of a strongly magnetic CV; IP = intermediate polar, i.e. coherent short-period variability related to the WD spin is detected; NL = nova-like variable, i.e. the system is in a persistent state of high mass transfer; CV = no confirmed CV subtype; EC = eclipsing. Two additional flags are given: WD = the SDSS spectrum is dominated by the WD, RASS = the system has been detected in the RASS.

SDSSJ	g	P_{orb} (min)	Type	WD	RASS	Reference
003941.06+005427.5	20.6	91.50(16)	CV	Y	N	IV,1
004335.14-003729.8	19.8	82.325(88)	CV	Y	N	III,2
005050.88+000912.7	20.4	80.3(2.2)	CV	Y	N	IV,3
013132.39-090122.3	18.3	81.54(13)	CV	Y	N	II,3
013701.06-091234.9	18.7	79.71(1)	DN	Y	N	II,4
015151.87+140047.2	20.3	118.68(4)	DN	N	N	I,5
015543.40+002807.2	15.4	87.143517(1)	AM/EC	N	Y	I,6,7,8
023322.6+005059.50	19.9	96.08(9)	IP:	N	N	I,9
031051.66-075500.2	22.3	95.9(2.0)∗	DN	N	N	II,10
032855.00+052254.2	18.0	121.97(25)	AM	N	N	VI
040714.78-064425.1	17.8	245.045(43)	DN/EC	N	N	II,11
074531.92+453829.6	19.0	76.00(16)	CV	Y	N	V,1
074640.62+173412.8	21.1	93.5(2.0)∗	DN	N	N	V,10
075059.97+141150.1	19.1	134.1530(39)	CV/EC	N	N	VI,1
075240.45+362823.2	17.7	164.4(3.0)	AM	N	N	II,12
075443.01+500729.2	17.3	205.965(14)	NL/EC	N	N	V,3
075507.70+143547.6	18.3	84.760(58)	CV	Y	N	VI,1
075939.79+191417.3	18.2	188.45(80)	CV	N	N	V,1
080215.38+401047.1	16.7	221.62(4)	NL	N	N	II,13
080434.20+510349.2	17.9	84.96(4)	DN	Y	N	V,14,15,16
080534.49+072029.1	18.5	330.8(9)	CV	N	N	VI,17
080846.19+313106.0	19.4	296.45(75)	DN	N	N	III,13
080908.39+381406.2	15.6	193.015(12)	NL/EC	N	N	II,18
081256.85+191157.8	15.8	230.4(3)	NL	N	N	V,17
081207.63+131824.4	19.3	116.8(2.0)∗	SU	N	N	VI,10
081321.91+452809.4	18.3	416.2(6)	DN	N	N	I,19
081352.02+281317.3	17.1	175.11(56)	CV	N	N	IV,17
082409.72+493124.4	19.3	95(3)	DN	N	N	I,5,20
083845.23+491055.4	19.6	99.7(2.0)∗	DN	N	N	I,10
084400.10+023919.3	18.3	298.1(7)	CV	N	N	II,17
090016.56+430118.2	18.9	301.492(78)	CV	N	N	III,1
090103.93+480911.1	19.3	112.147927(50)	DN/EC	N	N	II,5
090350.73+330036.1	18.8	85.065902(13)	CV/EC	N	N	IV,13,21
090403.48+035501.2	19.2	86.000(8)	CV	Y	N	III,22
091127.36+084140.7	19.7	295.74(22)	CV	N	N	IV,9
091945.11+085710.0	18.2	81.3(2)	CV	Y	N	IV,5,17
092009.54+004244.9	17.5	212.944(11)	CV/EC	N	N	II,23
092122.83+203857.0	19.8	84.2409(36)	AM	N	N	VII,1,24
092444.48+080150.9	19.3	131.2560(67)	AM:/EC	N	N	IV,1
093249.56+472523.0	17.8	95.47669(11)	CV/EC	N	N	III,13,25
100515.38+191107.9	18.2	107.6(2.0)∗	DN	Y	N	VII,10
100658.40+233724.4	18.3	267.7163(30)	CV/EC	N	N	VI,1
103100.55+202832.2	18.3	83.2(2.3)	AM	N	N	26
103533.02+055158.3	18.8	82.0897(3)	CV/EC	Y	N	V,9,21,27
110014.72+131552.1	18.7	94.5(2.0)∗	DN	N	Y	V,10
115207.00+404947.8	19.3	97.4(4)	CV/EC	Y	N	VI,1
121209.31+013627.7	18.0	88.428(1)	AM	Y	N	28,29,30
121607.03+052013.9	20.1	98.82(16)	CV	Y	N	III,9
122740.82+513924.9	19.1	90.64859(1)	DN/EC	Y	N	V,21,31
123813.73-033932.9	17.8	80.52(50)	CV	Y	N	II,32
124426.25+613514.5	18.8	142.9(2)	CV	N	Y	III,5
125023.84+665525.4	18.7	84.5793893(63)	CV/EC	N	N	II,5
132411.57+032050.4	22.1	158.72(9)	AM	N	N	III,1,33
132723.38+652854.3	17.8	196.772(89)	NL/EC	N	N	II,34
133941.11+484727.5	17.6	82.524(24)	CV	Y	N	IV,35
143317.78+101123.3	18.6	78.106578(3)	CV/EC	Y	N	IV,21
150137.22+550123.3	19.4	81.8513(3)	CV/EC	Y	N	III,21
150240.97+333423.8	17.6	84.82984(7)	CV/EC	N	N	V,21

Table 1 – *continued*

SDSSJ	g	P_{orb} (min)	Type	WD	RASS	Reference
150722.33+523039.8	18.3	66.612011(1)	CV/EC	Y	N	IV,21,36
152419.33+220920.0	19.1	94.1(1)	DN/EC	N	N	VII,37
153817.35+512338.0	18.6	93.11(9)	CV	N	N	III,13
154104.67+360252.9	19.7	84.3(3)	AM	N	N	IV,23
155331.11+551614.4	18.5	263.48(6)	AM	N	N	II,33
155531.99-001055.0	19.4	113.54(3)	CV/EC	N	N	I,3
155644.23-000950.2	18.1	106.675(14)	DN	Y	N	I,6,17
155656.92+352336.6	18.4	128	CV/EC	N	N	V
160745.02+362320.7	18.1	225.36(0.63)	NL/EC	N	N	V,13
161033.63-010223.3	19.1	80.52(8)	CV	Y	N	I,38,39
162718.39+120435.0	19.2	150(3)*	DN	N	N	VII,10,40
162936.53+263519.5	19.3	134(2)	AM	N	N	IV,23
163722.21-001957.1	20.6	97.04(19)	DN	N	N	I,2
164248.52+134751.4	18.6	113.6(1.5)	CV	N	N	VI,2
165359.05+201010.4	18.5	89.7(2.0)*	DN	N	N	V,23
165658.13+212139.3	18.5	90.89(15)	CV	N	Y	IV,17
165837.70+184727.4	20.1	98.012(65)	CV	N	N	V,2
170053.29+400357.6	19.4	116.3545(1)	AM	N	Y	II,12
170213.25+322954.1	17.9	144.118(1)	DN/EC	N	N	III,41,42
171145.08+301319.9	20.3	80.35(5)	CV	Y	N	III,5
173008.38+624754.7	16.3	110.22(12)	DN	N	N	I,37
204448.91-045928.7	16.9	2420(14)	CV	N	N	II,43
204817.85-061044.8	19.4	87.49(32)	CV	Y	N	II,13,44,45
205017.83-053626.7	18.1	94.21165(3)	AM	N	Y	II,6,46,47
205914.87-061220.5	18.4	107.52(14)	DN	N	N	II,3
210449.95+010545.9	20.4	103.62(12)	DN	N	N	II,3
211605.43+113407.3	22.5	80.2(2.2)	DN	N	N	III,5
215411.12-090121.6	19.2	319(3)	CV	N	N	II,5
210014.11+004445.9	18.7	120.8(2.0)*	DN	N	N	III,48
220553.98+115553.7	20.1	82.81(9)	CV	Y	N	II,49
223439.93+004127.2	18.1	127.29(25)	CV	N	N	II,13
225831.18-094931.6	15.7	118.9(2.0)*	DN	N	Y	II,10
230351.64+010651.0	19.1	110.51(24)	DN	N	Y	I,13
233325.92+152222.2	18.7	83.39(8)	IP	N	N	V,50

[I]Szkody et al. (2002c); [II]Szkody et al. (2003a); [III]Szkody et al. (2004); [IV]Szkody et al. (2005); [V]Szkody et al. (2006); [VI]Szkody et al. (2007a); [VII]Szkody et al. (2009); [1]Southworth et al. (in preparation); [2]Southworth et al. (2008b); [3]Southworth et al. (2007b); [4]Pretorius et al. (2004); [5]Dillon et al. (2008); [6]Woudt, Warner & Pretorius (2004); [7]Schmidt et al. (2005b); [8]O'Donoghue et al. (2006); [9]Southworth et al. (2006); [10]Kato et al. (2009); [11]Ak et al. (2005); [12]Homer et al. (2005); [13]Dillon et al. (in preparation); [14]Pavlenko et al. (2007); [15]Shears, Klingenberg & de Ponthiere (2007); [16]Zharikov et al. (2008); [17]Thorstensen et al. (in preparation); [18]Rodríguez-Gil, Schmidtobreick & Gänsicke (2007a); [19]Thorstensen, Fenton & Taylor (2004); [20]Boyd, Shears & Koff (2008); [21]Littlefair et al. (2008); [22]Woudt et al. (2005); [23]this paper; [24]Schmidt et al. (2008); [25]Homer et al. (2006a); [26]Schmidt et al. (2007); [27]Littlefair et al. (2006b); [28]Schmidt et al. (2005a); [29]Burleigh et al. (2006); [30]Farihi, Burleigh & Hoard (2008); [31]Shears et al. (2008); [32]Zharikov et al. (2006); [33]Szkody et al. (2003b); [34]Wolfe et al. (2003); [35]Gänsicke et al. (2006); [36]Littlefair et al. (2007); [37]Patterson et al. (in preparation); [38]Woudt & Warner (2004); [39]Copperwheat et al. (2009); [40]Shears et al. (2009); [41]Littlefair et al. (2006a); [42]Boyd, Oksanen & Henden (2006); [43]Peters & Thorstensen (2005); [44]Woudt et al. (2005); [45]Woudt, Warner & Pretorius (2009); [46]Potter et al. (2006); [47]Homer et al. (2006b); [48]Tramposch et al. (2005); [49]Southworth, Townsley & Gänsicke (2008a); [50]Southworth et al. (2007a).

CVs for which an SDSS spectrum that allows their identification as a CV is available in Data Release 6 (DR6, Adelman-McCarthy et al. 2007), independently of whether they were already known before or not. Furthermore, we shall call new SDSS CVs those systems that were genuinely identified from SDSS spectroscopy, and old SDSS CVs those systems which were known to be CVs beforehand, and were found again among the SDSS spectra. Finally, we shall call non-SDSS CVs all CVs from V7.6 of the Ritter & Kolb (2003) catalogue which have *no* spectrum in SDSS DR6, and excluding the systems which were flagged as having an uncertain orbital period measurement. The four different samples contain 454 (non-SDSS CVs), 137 (SDSS CVs), 92 (new SDSS CVs) and 45 (old SDSS CVs) systems.

Fig. 2 compares the orbital period distribution of 454 non-SDSS CVs and that of 137 SDSS CVs. The well-known features of the non-SDSS CV population are the deficiency of systems in the 2–3 h period gap, roughly equal numbers of systems above and below the gap, a minimum period near 80 min, and a drop-off of systems towards longer periods above the gap. In numbers, the non-SDSS CV sample contains 167, 48 and 239 systems with $P_{orb} \leq 2$ h, 2 h $< P_{orb} \leq 3$ h and $P_{orb} > 3$ h, respectively.

The period distribution of the SDSS CVs looks radically different compared to that of the non-SDSS CVs. The majority of the systems are found below the period gap, with 92, 17 and 28 systems below, in, and above the 2–3 h period gap, respectively, confirming the trend already noticed by Szkody et al. (2003a, 2007a) and Southworth et al. (2006, 2007b). The most striking feature is an apparent accumulation of systems in the shortest period bin. Comparing the orbital period distributions of the old SDSS CVs and the new SDSS CVs sample (Fig. 2, right-hand panel) indicates that the distribution

Table 2. Previously known CVs (old SDSS CVs), which were spectroscopically re-identified by SDSS. The definition of the columns are the same as in Table 1.

SDSSJ	Other name	SDSS g	P_{orb} (min)	Type	WD	RASS	Reference
002728.01−010828.5	EN Cet	20.7	85.44(7)	DN	Y	N	IV,1
075117.32+144423.9	PQ Gem	14.2	311.56(4)	IP	N	Y	V,2
075853.03+161645.1	DW Cnc	15.3	86.1015(3)	IP	N	N	V,3,4
082236.03+510524.5	BH Lyn	15.3	224.460831(20)	NL/EC	N	N	I,5,6,7,8
083619.15+212105.3	CC Cnc	16.8	105.86(7)	DN	N	Y	V,9
083642.74+532838.0	SW UMa	16.9	81.8136(1)	DN	N	Y	I,10,11
084303.98+275149.6	EG Cnc	18.9	85.5(9)	DN	Y	N	IV,12,13
085107.39+030834.3	CT Hya	18.8	93.9(2.0)*	DN	N	N	II,14,15
085344.16+574840.5	BZ UMa	16.4	97.8(1)	DN	N	Y	II,16
085414.02+390537.2	EUVE J0854+390	19.2	113.26(3)	AM	N	Y	IV,1
085909.18+053654.5	RX J0859.1+0537	18.6	143.8	AM	N	Y	IV,17
090950.53+184947.4	GY Cnc	16.4	252.6371983(30)	DN/EC	N	Y	VII,18,19
093214.82+495054.7	1H 0928+5004	17.5	602.45813(43)	NL/EC	N	N	V,20
093836.98+071455.0	PG 0935+075, HM Leo	18.3	269.0(4)	DN	N	N	IV,21
094431.71+035805.5	RXJ 0944.5+0357, VZ Sex	16.8	214.4(2)	DN	N	Y	II,19,22,23
094636.59+444644.7	DV UMa	19.4	123.6278190(20)	DN/EC	N	N	IV,24,25,26
101534.67+090442.0	GG Leo	17.2	79.879464(66)	AM	N	Y	IV,27
101947.26+335753.6	HS 1016+3412	18.4	92.22(17)	DN	N	Y	VI,28
102026.52+530433.1	KS UMa	17.4	97.86(14)	DN	N	Y	III,22,29
102320.27+440509.8	NSV 4838, UMa 8	18.8	97.8(3)	DN	N	N	IV,20
102800.07+214813.5	1H 1025+220	16.0	210.36	EC	N	N	VII,30
104356.72+580731.9	IY UMa	17.7	106.42892(7)	DN/EC	N	N	VII,31,32,33
105135.14+540436.0	EK UMa	18.4	114.5(2)	AM	N	N	IV,34
105430.43+300610.1	SX LMi	16.8	96.72(16)	DN	N	Y	VI,35,36
105656.99+494118.2	CY UMa	17.8	100.18(6)	DN	N	N	IV,37,38
110425.64+450314.0	AN UMa	15.8	114.84406(6)	AM	N	N	V,39,40
110539.76+250628.6	ST LMi	17.6	113.8882(1)	AM	Y	Y	VII,41
111544.56+425822.4	AR UMa	15.6	115.92107(17)	AM	N	N	V,42,43
113122.39+432238.5	RX J1131.3+4322, MR UMa	16.2	91.25(12)	DN	N	N	V,44
113722.24+014858.5	RZ Leo	18.7	109.6(2)	DN	Y	Y	II,29
113826.82+032207.1	T Leo, QZ Vir	14.9	84.6994(7)	DN	N	Y	II,45
114955.69+284507.3	EU UMa	17.9	90.14(2)	AM	N	Y	VII,46
115215.82+491441.8	BC UMa	18.5	90.16(6)	DN	Y	N	III,29
125637.10+263643.2	GO Com	18.3	95(1)	DN	N	Y	VII,47,48,49
130753.86+535130.5	EV UMa	16.5	79.687973(29)	AM	N	Y	IV,50,51
134323.16+150916.8	HS 1340+1524	17.6	92.66(17)	DN	N	Y	VII,28
143500.21−004606.3	OU Vir	18.6	104.696803(7)	DN/EC	N	N	I,52,53
151302.29+231508.4	NY Ser	16.4	140.4(3)	DN	N	N	VII,29,54
152613.96+081802.3	QW Ser	18.1	107.3(1)	DN	N	N	VII,29
155247.18+185629.1	MR Ser	17.2	113.4689(1)	AM	N	N	VII,55
155412.33+272152.4	RX J1554.2+2721, AP CrB	17.6	151.865(9)	AM	N	Y	VI,56,57
155654.47+210718.8	QZ Ser	17.9	119.752(2)	DN	N	N	VI,58
161007.50+035232.7	RX J1610.1+0352	17.7	190.54(6)	AM	N	Y	VII,59,60
162501.74+390926.3	V844 Her	17.2	78.69(1)	DN	N	Y	IV,61
223843.84+010820.7	Aqr 1	18.3	194.30(16)	IP	N	N	II,62,63,64

[I]Szkody et al. (2002c); [II]Szkody et al. (2003a); [III]Szkody et al. (2004); [IV]Szkody et al. (2005); [V]Szkody et al. (2006); [VI]Szkody et al. (2007a); [VII]Szkody et al. (2009); [1]Dillon et al. (2008); [2]Hellier, Ramseyer & Jablonski (1994); [3]Rodríguez-Gil et al. (2004); [4]Patterson et al. (2004); [5]Thorstensen et al. (1991); [6]Dhillon et al. (1992); [7]Hoard & Szkody (1997); [8]Stanishev, Kraicheva & Genkov (2006); [9]Thorstensen (1997); [10]Howell & Szkody (1988); [11]Shafter, Szkody & Thorstensen (1986); [12]Patterson et al. (1998); [13]Kato et al. (2004); [14]Nogami, Kato & Hirata (1996); [15]Kato et al. (1999); [16]Ringwald, Thorstensen & Hamwey (1994); [17]Reinsch, priv. comm.; [18]Gänsicke et al. (2000); [19]Feline et al. (2005); [20]Thorstensen (in preparation); [21]Thorstensen & Taylor (2001); [22]Jiang et al. (2000); [23]Mennickent et al. (2002); [24]Howell et al. (1988); [25]Patterson et al. (2000b); [26]Feline et al. (2004a); [27]Burwitz et al. (1998); [28]Aungwerojwit et al. (2006); [29]Patterson et al. (2003); [30]Taylor (1999); [31]Uemura et al. (2000); [32]Patterson et al. (2000a); [33]Steeghs et al. (2003); [34]Morris et al. (1987); [35]Nogami, Masuda & Kato (1997); [36]Wagner et al. (1998); [37]Martinez-Pais & Casares (1995); [38]Thorstensen et al. (1996); [39]Liebert et al. (1982); [40]Bonnet-Bidaud et al. (1996); [41]Cropper (1989); [42]Remillard et al. (1994); [43]Schmidt et al. (1999); [44]Patterson et al. (2005); [45]Shafter & Szkody (1984); [46]Howell et al. (1995a); [47]Howell, Szkody & Cannizzo (1995b); [48]Howell et al. (1990); [49]Howell, priv. comm.; [50]Osborne et al. (1994); [51]Katajainen et al. (2000); [52]Vanmunster, Velthuis & McCormick (2000); [53]Feline et al. (2004b); [54]Nogami et al. (1998); [55]Schwope et al. (1991); [56]Tovmassian et al. (2001); [57]Thorstensen & Fenton (2002); [58]Thorstensen et al. (2002a); [59]Schwope et al. (2002); [60]Rodrigues et al. (2006); [61]Thorstensen et al. (2002c); [62]Woudt et al. (2004); [63]Berg et al. (1992); [64]Southworth et al. (2008b).
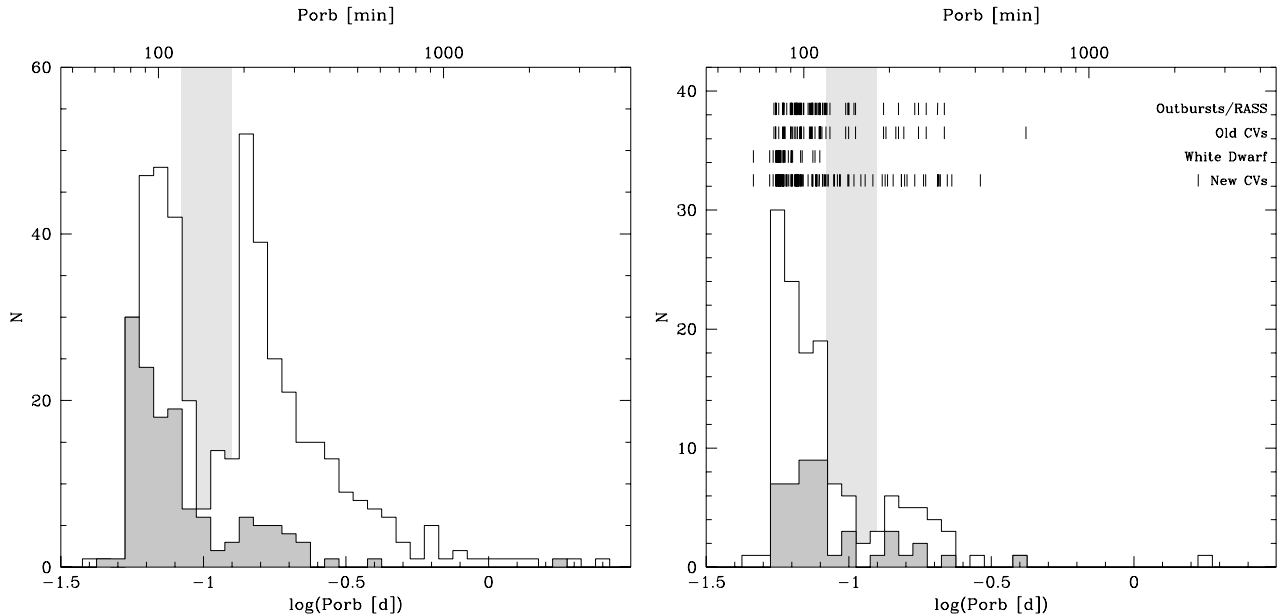
Figure 2. Left-hand panel: The orbital period distribution of 454 CVs from Ritter & Kolb (2003), V7.6, which have no spectroscopic observation in SDSS DR6 (white) and the distribution of 137 SDSS CVs from Tables 1 and 2 (SDSS CVs, grey). The grey shaded area represents the 2–3 h orbital period gap. These distributions exclude the hydrogen-deficient AM CVn systems. Right-hand panel: the period distribution of the SDSS CVs divided into 45 previously known systems (old SDSS CVs, grey) and 92 newly identified CVs (new SDSS CVs, white). Superimposed are tick marks indicating the individual orbital periods of the old and new SDSS CVs, along with the periods of SDSS CVs showing outbursts and/or being detected in the RASS, and the distribution of the periods of the SDSS CVs which clearly reveal the WD in their optical spectra. The bin width in both panels is 0.05 log(d).

of the old SDSS CVs is flat below the period gap, and that the 'spike' at the orbital period minimum comes entirely from the new CVs identified by SDSS.

Cumulative period distributions of the non-SDSS CVs, the old SDSS CVs and the new SDSS CVs are shown on a linear scale in orbital period in Fig. 3. The large number of new CVs among the

Figure 3. Normalized cumulative period distributions in the range $P_{orb} = 76$–120 min of (a) 454 CVs from Ritter & Kolb (2003; V7.6), excluding systems with spectroscopy in SDSS DR6 and systems whose periods are marked as uncertain (black), (b) 45 previously known CVs recovered from SDSS spectroscopy (red) and (c) 92 new CVs identified from SDSS spectroscopy (blue). A two-sided KS test comparing the distributions of the non-SDSS CVs and the new SDSS CVs results in a 9.5×10^{-3} probability for the two distributions being drawn from the same parent population. In contrast, the probability that the non-SDSS CVs and the previously known SDSS CVs are drawn from the same sample is 57.4 per cent.

new SDSS CVs near the period minimum is reflected in the rapid rise of the cumulative distribution over the range $\sim$80–86 min, with a clear break in slope at $\sim$86 min. In Section 4, we will inspect the properties of the systems in this $\sim$80–86 min period spike.

We have applied a two-sided Kolmogorov–Smirnov (KS) test in order to test whether the three cumulative distributions deviate from one another in a statistically significant way. As a lower limit, we chose 76.78 min, corresponding to the shortest-period 'standard' hydrogen-rich CV, GW Lib.[3] We set the upper period limit for the KS test to 120 min, i.e. the lower edge of the period gap. The reason for this choice is that CVs with periods above the gap have substantially brighter absolute magnitudes compared to the short-period systems, and hence SDSS, sampling the sky at high Galactic latitudes, $|b| > 30°$, will be biased against the detection of long-period CVs.[4] In fact, a substantial fraction of previously known long-period CVs contained in the SDSS footprint are saturated in the SDSS imaging data, were consequently not selected by the
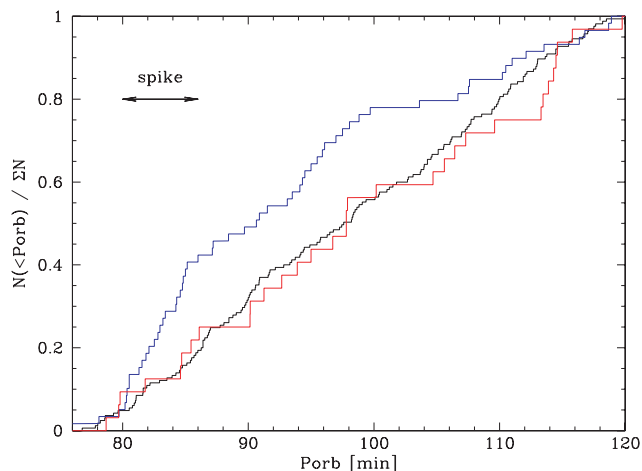
---

[3] Three hydrogen-rich CVs with orbital periods around 60 min are known: V485 Cen, EI Psc and SDSS J1507+5230. The evolutionary state of these systems is not entirely clear, EI Psc contains an evolved donor star (Thorstensen et al. 2002b) and SDSS J1507+5230 may have formed with a brown dwarf donor (Littlefair et al. 2007) or be a halo CV (Patterson, Thorstensen & Knigge 2008). For the discussion of the SDSS CV period distribution, we decided to exclude these three oddball systems.

[4] Examples of luminous CVs above the period gap are TT Ari, with $P_{orb} = 198.07$ min, $V \simeq 10.6$ and $d = 335 \pm 50$ pc (Thorstensen, Smak & Hessman 1985; Gänsicke et al. 1999), and MV Lyr with $P_{orb} = 191.4$ min, $V \simeq 12.0$ and $d = 505 \pm 50$ pc (Skillman, Patterson & Thorstensen 1995; Hoard et al. 2004), corresponding to absolute magnitudes of $M_V = 3.0 \pm 0.3$ and 3.5 ± 0.2, respectively. At $|b| = 30°$, SDSS could detect these systems out to >10 kpc above the Galactic disc. See Section 5.1 for details on the sky volume coverage of SDSS.

SDSS target algorithms for spectroscopic follow-up, and are hence not available in the SDSS CV sample.

The KS test comparing the cumulative period distributions of the non-SDSS CVs and the new SDSS CVs results in a 9.5×10^{-3} probability that the two distributions are randomly drawn from an identical parent population, which shows that the period distribution of the new SDSS CVs differs significantly from that of the previously known CV sample. This clearly suggests that the CV identification within SDSS differs from the average CV discovery method in the previously known sample.

Conversely, comparing the cumulative period distributions of the non-SDSS CVs and the old SDSS CVs, the probability for both distributions emanating from the same parent sample is 57.4 per cent, i.e. the two distributions are identical from a statistical point of view. This is not surprising, as the old CVs have been identified by the same methods as the non-SDSS CVs, i.e. primarily dwarf nova outbursts and X-ray emission.

We conclude for now that the orbital period distributions of the new SDSS CVs and of the previously known CVs (independently of whether or not they were also selected by SDSS for spectroscopic follow-up) differ significantly, most apparently in the ratio of the number of short- and long-period systems, and in the appearance of a spike at $\sim$80–86 min in the period distribution of the new SDSS CVs. In the next section, we will discuss in more detail additional differences between the new SDSS CV and non-SDSS CV samples.

4 PROPERTIES OF THE PERIOD SPIKE CATACLYSMIC VARIABLES FOUND BY SDSS

As shown in Section 3, the orbital period distributions of the non-SDSS CVs and the new SDSS CVs differ at a $> 2.6\sigma$ level. This raises the question of whether the new SDSS CVs also differ in other properties besides their orbital period from the non-SDSS CVs. For the discussion below, we have defined the following three boolean characteristics: (i) the WD is clearly visible in the SDSS identification spectrum, (ii) X-ray emission has been detected in the *ROSAT* All Sky Survey (RASS; Voges et al. 2000)[5] and (iii) an optical outburst has been observed, leading to the classification as a dwarf nova.[6] Obviously, the non-detection of X-rays or outbursts is only an average characteristic, as the observations of an individual system may have just missed such activity. Tables 1 and 2 list these three properties for the 137 SDSS CVs with accurate orbital period measurements. Below, we will interpret the detection of the WD in the optical spectrum as evidence for a low mass transfer rate, and the detection of X-ray emission and/or outbursts as evidence of accretion activity which may lead to the identification of a system as a CV.

[5] While a number of SDSS CVs have been detected in pointed *ROSAT* observations, we restricted our assessment of X-ray emission to a detection in the RASS, as inclusion of pointed observations would imply wildly different X-ray flux limits for random lines-of-sight.

[6] Information on large-amplitude (>1 mag) variability has been drawn from three sources of information. (1) Brightness differences between the SDSS imaging and spectroscopic data, (2) individual follow-up observations which caught some systems in outburst (e.g. Tramposch et al. 2005; Southworth et al. 2007b; Dillon et al. 2008), and from the mailing lists of the amateur astronomers (vsnet, cvnet, baavss). We do *not* include outburst information from robotic telescopes, e.g. the Catalina Real-Time Transient Survey (Drake et al. 2009), *unless* they were announced via one of the appropriate mailing lists.
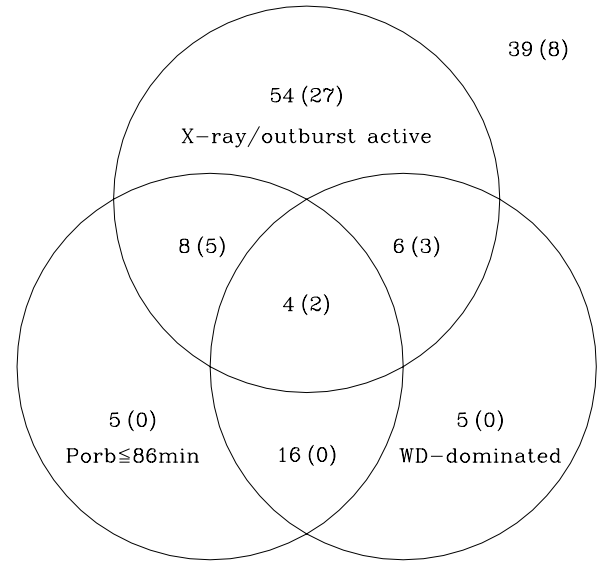

Figure 4. Venn diagram showing the distribution of 98 SDSS CVs with accurate orbital periods (Tables 1 and 2) into the following three categories: '$P_{orb} \leq 86$ min', 'has outbursts and/or has been detected in the RASS' and 'its optical spectrum is dominated by the WD'. The numbers in brackets refer to the properties of the previously known CVs that were re-identified by SDSS. Not all the systems from Table 1 are represented in this diagram, 39 additional SDSS CVs from Tables 1 and 2 have $P_{orb} > 86$ min, do not exhibit the WD in their SDSS spectra, and neither been detected in the RASS, nor seen in outburst.

In Fig. 4, we visualize the properties of the SDSS CVs in the form of a three-set Venn diagram, dividing them into systems with (1) $P_{orb} \leq 86$ min (i.e. within the period spike), (2) systems which reveal the WD in the SDSS identification spectrum and (3) systems which were detected in X-rays and/or outburst. The numbers for the previously known systems are given in parentheses. An immediate result from inspection of Fig. 4 is that all the previously known systems show accretion activity, whereas 26 of the new SDSS CVs have not been detected in the RASS and have not (yet) been detected in outburst so far.

Fig. 4 clearly illustrates that a large fraction (20/33) of the systems with orbital periods in the 80–86 min spike have optical spectra dominated by the WD. This generally indicates that the accretion disc and secondary star are dim and hence that the donor star is of a late spectral type and of low mass, and that the mass transfer rate is low. Of the systems not revealing their WDs, eight exhibit accretion activity, which is (on average) indicative of somewhat higher mass transfer rates than in the WD-dominated systems, and result in the WD being outshone by the accretion disc/stream. In fact, five of these eight systems were discovered because of their outbursts or X-ray emission (SW UMa, GG Leo, T Leo, EV UMa and V844 Her). The remaining three are the polar SDSS J1541+2721, and the dwarf novae SDSS J1250+6655 and SDSS J2116+1134. In magnetic CVs, the WD is typically not detected during states of active accretion, SDSS J1250+6655 is an eclipsing system, where the WD may be obstructed by the accretion disc, and the spectrum of SDSS J2116+1134 is too poor to make a definite judgement on the presence of broad WD absorption lines.

The very distinct spectral appearance between the CVs with $P_{orb} \leq 86$ min which are accretion-active and those which are not is demonstrated in Fig. 5, where four representative spectra from each group are shown. Clearly, the four old (accretion-active) SDSS CVs
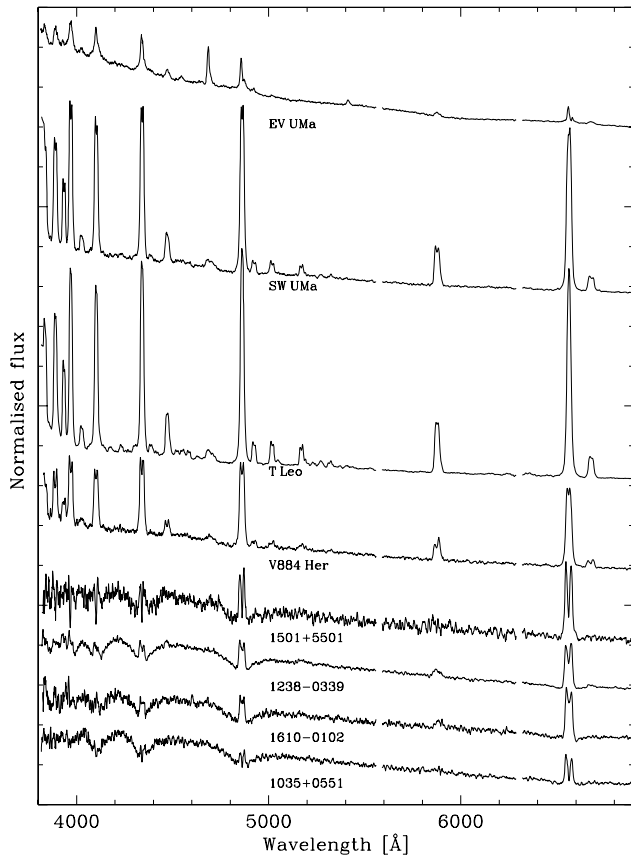
Figure 5. SDSS CVs with periods below 86 min. The top four objects are previously known systems re-identified by SDSS (old SDSS CVs, Table 2), the bottom four spectra are new identifications (new SDSS CVs, Table 1).

EV UMa, SW UMa, T Leo and V884 Her have strong Balmer and He I emission lines, or He II in the case of the polar EV UMa. These four systems have been identified as an X-ray emitter (EV UMa) and as outbursting dwarf novae (SW UMa, T Leo, V884 Her). The four WD-dominated new SDSS CVs, SDSS J1501+5501, SDSS J1238−0339, SDSS J1610−0102 and SDSS J1035+0551, have moderate to weak Balmer emission lines with a steep decrement, and hardly any He I emission, indicating lower temperatures and emission measures in their accretion flows than in the accretion-active CVs. SDSS J1501+5501 and SDSS J1035+0551 have dwarf donor stars with substellar masses (Littlefair et al. 2006b, 2008), indicating that they are probably highly evolved CVs, and the WD in SDSS J1610−0102 exhibits ZZ Ceti pulsations (Woudt & Warner 2004), which implies a relatively cool WD and a low secular mean accretion rate (Townsley & Bildsten 2003; Arras, Townsley & Bildsten 2006).

In addition to the eight accretion-active CVs with $P_{orb} \leq 86$ min where the WD cannot be detected in their SDSS spectra, there are another five systems that fail to reveal the WD and have also not been detected in X-rays and/or outburst. Two of these systems are eclipsing (SDSS J0903+3300 and SDSS J1502+3334). Given that the strength of emission lines is positively correlated with inclination (Warner 1986), the WD Balmer absorption lines are likely to be filled in by emission from the optically thin accretion flow and/or the WD might be veiled by the accretion disc altogether (Horne et al. 1994; Knigge et al. 2000). The other three systems are magnetic CVs

(SDSS J1031+2028, SDSS J0921+2038 and SDSS J2333+1522), where the WD is typically not seen during accretion-active phases.

Of particular interest are the four systems with $P_{orb} \leq 86$ min which are accretion-active, and do reveal the WD in their optical spectra: the two previously known systems EG Cnc (a well-studied WZ Sge-type dwarf nova) and EN Cet (a poorly studied dwarf nova), and the two new SDSS dwarf novae SDSS J0137−0912 (with a single observed superoutburst) and SDSS J0804+5103 (a WZ Sge dwarf novae with the first outburst observed in March 2005). All four systems are characterized by long outburst recurrence times, which is a signature of CVs with low mass transfer rates, and consistent with the detection of their WDs in the SDSS spectra.

A final note on Fig. 4 is that only 11 out of 104 SDSS CVs with $P_{orb} > 86$ min have WD-dominated optical spectra, confirming that the detection of the WD is indeed a spectroscopic fingerprint of the shortest period CVs.

Two additional properties of SDSS CVs with periods below 86 min are worth mentioning, as they again suggest a predominance of low-accretion rates and low-mass companion stars near the period minimum. (1) A number of non-radial WD pulsators have been identified by SDSS. For six of them accurate orbital periods have been measured, and with the exception of the ultra-short period system SDSS J1507+5230 (Patterson et al. 2008), they all reside within the 80–86 min period spike (Woudt & Warner 2004; Woudt et al. 2005; Gänsicke et al. 2006; Nilsson et al. 2006; Mukadam et al. 2007). If a sufficient number of pulsation mode frequencies can be identified, it will be possible to measure the WD core and envelope masses in these systems (Townsley & Bildsten 2003; Townsley & Gänsicke 2009). Obviously, the identification of WD pulsations relies in the first place on the clear detection of the WD in the optical wavelength range. In contrast to single WDs, where pulsators occupy a well-defined instability strip in the ($\log g$, T_{eff}) plane (Mukadam et al. 2004; Gianninas, Bergeron & Fontaine 2006), the temperatures of the pulsators in CVs span a relatively large range in effective temperature (Szkody et al. 2002a; Araujo-Betancor et al. 2005b; Szkody et al. 2007b). Theoretical work suggests that the presence of helium in the accreted material may result in additional driving mechanisms (Arras et al. 2006). (2) Three of the four SDSS CVs with confirmed donor stars with substellar masses are located within the period spike (SDSS J1035+0551, SDSS J1433+1011 and SDSS J1501+5501; Littlefair et al. 2006b, 2008);[7] these are probably CVs that have evolved past the period minimum.

In summary, 20 of the 33 SDSS CVs in the 80–86 min period spike are systems that differ dramatically from the bulk of the previously known short-period CVs: their SDSS spectra are dominated by emission from the WD, no spectroscopic signature from the companion star is evident at optical wavelengths, and very few exhibit obvious accretion activity such as X-ray emission or dwarf nova outbursts. All these characteristics suggest that these systems have very low accretion rates, and they are most likely all WZ Sge-type dwarf novae with extremely long recurrence times. Among the WD-dominated CVs discovered by SDSS, SDSS J0804+5103 is so far the only one to have revealed itself as a WZ Sge star (Pavlenko et al. 2007).

---

[7] The fourth confirmed brown dwarf donor has been found in SDSS J1507+5230 (Littlefair et al. 2007; Patterson et al. 2008), which has been excluded from the discussion in this paper as it has an orbital period of 66.6 min, way below the period minimum for 'standard' hydrogen-rich CVs.

5 DISCUSSION

We have shown in Section 3 that the period distribution of the SDSS CVs differs dramatically from that of the previously known CVs, with a substantially larger fraction of below-the-gap to above-the-gap systems, and a significant accumulation of CVs at the orbital period minimum. More specifically, the origin of the 80–86 min period spike is entirely due to the new CVs identified in SDSS, and, as outlined in Section 4, the systems in the period spike differ also in spectral morphology and accretion activity from the longer period CVs. Here, we will discuss why the CVs in the SDSS sample differ so clearly from the previously known systems, in particular the effects of survey depth and CV candidate selection.

5.1 Deep, deeper, the deepest

One very obvious difference between the SDSS CVs and CV samples from previous surveys is the unrivalled depth of Sloan. Hence, SDSS should be able to identify systems that were intrinsically too faint, or at too large a distance, for the previous surveys. This raises the question *does SDSS find more short-period CVs than previous surveys, such as the PG Survey or the HQS, just because of its depth?* A full treatment of this question would require the computation of a Galactic model of the CV population, which would need to be folded through the details of the sky coverage, magnitude limit and colour cuts of the considered surveys (see Pretorius, Knigge & Kolb 2007 for an analysis of this kind for the PG Survey). Given the intricate allocation algorithms for spectroscopic fibres within SDSS, this task is beyond the scope of the present paper (see, however, Section 5.2.1 for a brief discussion on the colour–colour exclusion boxes of the quasar target algorithm). For simplicity, we develop here an empirical comparison between SDSS, the HQS and the PG Survey, using their *effective survey volumes* for the WD-dominated systems near the period minimum. The effective survey volume is calculated by integrating over a spherical cap in Galactic coordinates covering Galactic latitudes higher than $|b_{lim}|$, weighting the volume by an exponential drop-off in the space density of CVs along the z-axis, with a scaleheight H_z. We assume radial symmetry around the z-axis in both the distribution of CVs and the coverage of the survey. Any more realistic work would need to account for the dependence of the CV space density on Galactic longitude, plus the exact tiling of the different surveys, as none of them covers the full spherical cap. Finally, the effective volume is weighted by the survey area.

The scaleheight is a poorly determined parameter, and we will assume in the following two values for H_z. The first one is the canonical value $H_z = 190$ pc introduced by Patterson (1984), broadly supported by Thomas & Beuermann (1998), who found $H_z = 155$ pc for strongly magnetic CVs, and Ak et al. (2008) who found $H_z = 128$–160 pc. The second value adopted below is $H_z = 260$ pc, following the argument of Pretorius et al. (2007) that old (short-period) CV populations are expected to have a larger scaleheight than younger objects. van Paradijs, Augusteijn & Stehle (1996) determined $H_z = 160$–230 pc from an analysis of the systemic velocity distribution of CVs, and concluded that CVs are an old disc population, with a mix of ages up to 10 Gyr. Pretorius et al. (2007) adopt $H_z = 450$ pc for period bouncers, being the oldest CVs, however, given the fact that there is little evidence of a period bounce population in the SDSS CV sample, we will not make use of such a large value for H_z.

We start with an estimate of the absolute magnitudes of the period minimum CVs, which we need to turn the magnitude limits of the surveys into distance limits, followed by a brief summary of the

survey characteristics, and then delve into the actual comparison of their results in terms of CV discoveries.

5.1.1 Absolute magnitudes of the period minimum cataclysmic variables

Unfortunately, the absolute magnitudes of CVs are notoriously poorly determined, as there are too few systems with accurate distance determinations to carry out a reliable calibration. With this caveat in mind, we will now compare the absolute magnitudes of the WD-dominated CVs found by SDSS to those of the previously known systems with $P_{orb} \leq 86$ min.

Among the seven old SDSS CVs with $P_{orb} \leq 86$ min (Table 2), there is just one system with a trigonometric parallax, the dwarf nova T Leo (Thorstensen 2003). From $d = 101^{+13}_{-11}$ pc and $g = 14.9$ we find $M_g = 9.9 \pm 0.3$. For SW UMa and EG Cnc spectral modelling of the WD in ultraviolet *HST*/STIS resulted in distance estimates of $d = 159 \pm 22$ and 420 ± 65 pc (Szkody et al. 2002b; Gänsicke et al. 2005), respectively, which results in $M_g = 10.9$ and 10.8, respectively. Taking the average over these three systems, we find $\langle M_g \rangle = 10.5 \pm 0.5$.[8]

Distance estimates are available for 13 of the WD-dominated new SDSS CVs in the period minimum spike: six from modelling high-speed light curves (Littlefair et al. 2008), four from modelling the optical SDSS spectra (Gänsicke et al. 2006; Mukadam et al. 2007) and three from modelling combined optical SDSS plus ultraviolet *HST*/ACS spectra (Szkody et al. 2007b). The resulting absolute magnitudes range from $M_g = 10.5$–13.1, with an average of $\langle M_g \rangle = 11.6 \pm 0.7$. The large spread is likely to be caused by the systematic uncertainties inherent to the distance determinations, rather than substantial intrinsic differences in the system properties. An independent check on these values can be obtained by considering that the WDs in these systems have typically $T_{eff} \simeq 12000$–15 000 K (Gänsicke et al. 2006; Mukadam et al. 2007; Littlefair et al. 2008). Assuming an average mass of 0.85 M$_\odot$ (Littlefair et al. 2008), and using an updated version of the photometric WD calibrations by Bergeron, Wesemael & Beauchamp (1995), we obtain $M_g = 12.2$–11.8 for the WDs alone. Given that, by definition, the WD is dominating the optical spectrum in these systems, adding a maximum of 50 per cent accretion luminosity to the brightness results in $M_g = 11.3$–11.7 for the bulk of the new SDSS CVs in the period minimum spike, entirely consistent with our estimate of $\langle M_g \rangle = 11.6 \pm 0.7$.

While not statistically significant, the absolute magnitudes derived above suggest that the new SDSS CVs are on average intrinsically fainter than the old SDSS CVs, which is not too surprising as the mere fact that the WD is the dominant source of light implies that the accretion luminosity is low. It is interesting to compare our numbers here with the work of Patterson (1998), who estimated time-averaged absolute magnitudes for a large number of CVs, finding a nearly flat distribution between $M_V = 4$–11, with a sharp cut-off for fainter systems. The faintest bin in Patterson's (1998) fig. 2 is populated only by a handful of WZ Sge type dwarf novae, and it is in that bin that the WD-dominated CVs (which are

---

[8] For completeness, the polars EV UMa and GG Leo have lower limits on their distances, $d \gtrsim 705$ pc and $d > 100$ pc (Osborne et al. 1994; Burwitz et al. 1998), which give $M_g \lesssim 7.3$ and $\lesssim 12.2$, respectively. However, such lower limits on distances are very uncertain due to the possible contamination by cyclotron emission, and we do not include these two systems in our analysis above.

presumably all WZ Sge type dwarf novae) will slot in. However, Patterson's (1998) statement '...*with not a single star fainter than* $\langle M_v \rangle = 11.6$' still holds, as no system significantly fainter than that limit has been found by SDSS.

5.1.2 Sloan Digital Sky Survey

The SDSS covers high Galactic latitudes, $|b| > 30°$ (York et al. 2000). Within the main quasar search, spectroscopic follow-up is carried out on point-sources with colours different from those of main-sequence stars and a limiting magnitude of a (Galactic column) de-reddened $i = 19.1$ for ultraviolet excess/low-redshift quasars and of a de-reddened $i = 20.2$ for high-redshift ($z \gtrsim 3$) quasars (Richards et al. 2002). The detailed fibre allocation algorithm is complex, and we will assume for the moment that the completeness in the follow-up of blueish CVs within the magnitude limits is as high as that for the targeted ultraviolet excess quasars (~90 per cent, Schneider et al. 2007, see Section 5.2.1 below). Further, we assume a typical Galactic reddening of $E(B - V) = 0.05$, which translates into a reddening correction in i of 0.1 mag, increasing the observed magnitude limit of the low-redshift quasar survey to $i = 19.2$. The WD-dominated CVs have on average $\langle g - i \rangle \simeq -0.2$, which leads to a limiting magnitude for such systems within the main quasar survey of $g \simeq 19.0$. Using $\langle M_g \rangle = 11.6$ as determined above, this implies that SDSS should be able to serendipitously identify WD-dominated systems out to $d = 302$ pc. Given that Szkody et al. (2007a) published some CVs beyond DR5, and we include here in addition to her lists (Szkody et al. 2002c to Szkody et al. 2007a) the previously known CVs within DR6, we assume a survey area for the spectroscopic SDSS data base of 6400 deg^2, which is in between the official DR5 and DR6 areas.

5.1.3 Hamburg Quasar Survey

The HQS is another high-Galactic latitude ($|b| > 20°$) survey covering 13 600 deg^2 with a typical limiting magnitude of $B = 17.5$. Using the colour transformations of Jester et al. (2005), the HQS has a limiting magnitude of $g \simeq 17.4$ for blue objects. Spectroscopic follow-up over the wavelength range 3400–5400 Å was obtained

by means of Schmidt prism spectroscopy, which is hence complete except for plate artefacts or blends. About 50000 blue objects with $U - B \lesssim -0.5$ were extracted from the photographic plates and visually classified. Objects with Balmer emission lines were selected as CV candidates for detailed follow up (Gänsicke et al. 2002; Aungwerojwit et al. 2006). Given the average colour of the WD-dominated CVs found in SDSS of $\langle u - g \rangle \simeq 0.15$, the HQS should be able to identify such systems out to $d = 145$ pc.

5.1.4 Palomar Green Survey

The PG Survey extended over 10 714 deg^2 at Galactic latitudes $|b| > 30°$ with spectroscopic follow-up for 1874 objects (Green, Schmidt & Liebert 1986). The survey design was a blue-cut of $U - B < -0.46$ and a typical limiting magnitude of $B < 16.1$. Comparison with SDSS data in overlapping areas showed however that the PG Survey had a rather bluer cut of $U - B < -0.71$ (Jester et al. 2005). Using the colour transformation from Jester et al. (2005), the PG colour cut and limiting magnitude are $u - g < 0.3$ and $g = 16.1$. Hence the PG Survey should be able to identify short-period CVs out to $d = 79$ pc.

5.1.5 Finding period minimum cataclysmic variables: a comparison of SDSS, HQS and PG

Using the survey characteristics summarized above, we calculated the effective survey volumes for finding period minimum CVs, as outlined above, for the SDSS, HQS and PG Survey. As we are only interested in the relative 'catchment area', we normalize all numbers to the effective volume of the main quasar survey within SDSS, i.e. to SDSS with a limiting magnitude of $g = 19.0$, and report the resulting numbers in Table 3. Along with the normalized effective volumes, we list in Table 3 the number of CVs with $P_{orb} \leq 86$ min identified by each survey, and in a separate column the number of those period minimum CVs in which the WD is detected in their optical spectra. For the case of SDSS, we give three additional subsamples with the following limiting magnitudes: (a) $g_{lim} = 22.5$, which is the magnitude of the faintest SDSS CV, resulting in the most inclusive sample of systems, and (b) $g_{lim} = 17.4$ and $g_{lim} = 16.1$, which will allow investigation of how SDSS compares

Table 3. Comparison of the SDSS, HQS and PG Survey in terms of their potential for discovering period minimum CVs. The first three columns give the magnitude limit, sky coverage and Galactic latitude range for the three surveys. For SDSS, we defined subsamples with different limiting magnitudes. $g_{lim} = 22.5$ corresponds to the full CV sample, $g_{lim} = 19.0$ includes all CVs within the magnitude limit of the low-redshift quasar survey, and $g_{lim} = 17.4$ and 16.1 are selected to compare SDSS like-for-like with the HQS and the PG Survey. From these characteristics, we calculated an effective survey volume for WD-dominated CVs as outlined in Section 5.1. The survey volumes were calculated for two different assumptions of the scaleheight, H_z, of the CV population, and normalized to the volume of the SDSS low-redshift quasar survey ($g_{lim} = 19.0$). The last two columns give the number of all CVs with $P_{orb} \leq 86$ min found in the three surveys, and the number of period minimum CVs with WD-dominated spectra. Numbers following a '/' are normalized to the SDSS values.

Survey	g_{lim}	d_{lim} (pc)	Area (deg^2)	$|b|$	V_{norm} $H_z = 190$ pc	$H_z = 260$ pc	$N_{CV}(P_{orb} \leq 86$ min) All CVs	WD-dominated
SDSS	22.5	1514	6400	>30°	1.36	4.11	33/1.57	20/1.81
	19.0	302			1.00	1.00	21/1.00	11/1.00
	17.4	145			0.24	0.20	5/0.20	0/0.00
	16.1	79			0.05	0.04	1/0.0	0/0.00
HQS	17.4	145	13600	>20°	0.50	0.40	6/0.27	1/0.08
PG	16.1	79	10714	>30°	0.08	0.05	3/0.14	1:/0.08

with the HQS and the PG Survey if operating at the same limiting magnitude.

The first thing to note is that the difference in effective survey volumes depends only mildly on the different assumption for the scaleheight, the reason being that both HQS and PG are so shallow that they do not even extend beyond one scaleheight, and hence do not feel much of the exponential drop-off in the CV space density.

SDSS beats the HQS in terms of survey volume only by about a factor two, which is due to the HQS covering more than twice the area on the sky, and extending down to lower Galactic latitudes. While the number of period minimum CVs found in the HQS is only slightly below the expectation from simply scaling the survey volume, it has only produced one WD-dominated CV (V445 And, Araujo-Betancor et al. 2005b), which is far below the expectations from its survey volume, suggesting a selection effect against the detection of such systems. Gänsicke et al. (2002) showed that the HQS is very efficient in finding short-period CVs similar to those known in the late 1990s, if they had Hβ equivalent widths in excess of $\sim$10 Å. Those were all CVs with substantial accretion luminosity such as SW UMa or T Leo, as only very few WD-dominated CVs were known at that time. However, Gänsicke et al. (2002) noted that the results from the HQS '*. . . exclude the presence of a large population of nearby infrequently outbursting X-ray faint short-period CVs unless they have significantly weaker emission lines than, e.g. WZ Sge'*. It turns out that those types of systems, short-period CVs with no or very rare outbursts, no or very weak X-ray emission, and weak Hβ equivalent widths are frequent among the CV catch of SDSS (Fig. 5). The difficulty in finding that type of system in the HQS was exacerbated by the low spectral resolution, averaging over the broad WD absorption lines and the weak emission lines, and thus even further decreasing the net equivalent widths of the Balmer emission.

Comparing SDSS and the PG Survey, the numbers of short-period CVs found are roughly in line with the expectations from the scaled survey volumes – only three CVs with $P_{\rm orb} \leq 86$ min were found, of which one may be WD dominated.

A final point of our comparison is to inspect whether, with regard to finding CVs near the period minimum, SDSS is a superset of the three surveys under inspection. The six CVs with $P_{\rm orb} \leq 86$ min in the HQS are SW UMa, T Leo, DW Cnc and HT Cam, all of which were previously known CVs with substantial accretion activity (outbursts/X-ray emission), and the two new discoveries KV Dra (HS1449+6415), an SU UMa type dwarf nova with rare outbursts and weak X-ray emission (Jiang et al. 2000; Nogami et al. 2000), and V455 And (HS2331+3905), the only WD-dominated period minimum CV in the HQS (Araujo-Betancor et al. 2005b). The first superoutburst of V455 And was observed in September 2007, confirming it as a WZ Sge type dwarf nova with a superoutburst cycle >5 years. Of those six period minimum systems in the HQS only T Leo, SW UMa, DW Cnc are in the footprint of SDSS DR6, and all were spectroscopically followed up by SDSS and, hence, (re-)identified as CVs.

The PG Survey contains three systems with $P_{\rm orb} \leq 86$ min: the previously known T Leo, and the PG discoveries RZ LMi and MM Hya (Green et al. 1982). RZ LMi is an SU UMa star with an ultra-short outburst cycle (Nogami et al. 1995; Robertson, Honeycutt & Turner 1995), which is thought to reflect an unusually high mass transfer rate for its orbital period (Osaki 1995a,b). MM Hya is a relatively poorly studied dwarf nova with rather rare outbursts (Ringwald 1993; Misselt & Shafter 1995). The spectrum published by Zwitter & Munari (1996) is of low quality, but suggests that MM Hya may be a WD-dominated CV similar to those

discovered in large number by SDSS. T Leo and RZ LMi are in the footprint of SDSS DR6, but only T Leo has been followed up spectroscopically. RZ LMi was found in the SDSS imaging at $g = 14.6$, close to the bright end where SDSS does follow-up observations, and was rejected by the quasar target selection algorithm.

In summary, comparing the numbers of period minimum CVs found in SDSS, the HQS and the PG Survey with the normalized effective survey volumes shows that the three surveys produce broadly consistent results. The main gain that SDSS brings over the previous surveys comes from its depth, and the massive spectroscopic follow-up of CV (and quasar) candidates.

5.2 Caveats?

Here, we discuss a number of possible caveats that could affect our conclusions about the period distribution of SDSS CVs made above.

5.2.1 The exclusion boxes in the SDSS quasar target selection

The decision on whether or not a photometric SDSS object will be allocated a fibre for spectroscopic follow-up is very complex, as a variety of science programs share the available resources. Because of their composite nature (WD, companion star, accretion flow), the colours of CVs in *ugriz* space differ markedly from those of single main-sequence stars or WDs. A detailed analysis of the spectroscopic completeness of SDSS as a function of location in *ugriz* colour space and apparent magnitude is in preparation and will be presented elsewhere. Here, we focus on the question *could the exclusion boxes in the SDSS quasar target selection algorithm cause a significant bias in the composition of the SDSS CV sample?* Early during the operations of SDSS, it became clear that the population of ultraviolet-excess quasars overlaps in *ugriz* colours space with WDs, resulting in a substantial stellar contamination of the quasar sample in these regions (Richards et al. 2002). Three *ugriz* exclusion boxes were defined to suppress the contamination of WDs, A-stars, and WD plus main-sequence (WDMS) binaries. Fig. 6 shows these colour exclusion boxes along with locations of single stars, quasars, and of the CVs from Tables 1 and 2. While excluded from the quasar candidate follow-up, a sufficient number of objects within these colour boxes were still observed within other SDSS science programs to establish their typical nature. The only SDSS CVs discussed in this paper contained in the WD exclusion box are SDSSJ 2116+1134 and SDSSJ 0310−0755 (none of which is WD dominated), which is a simple consequence of the fact that Balmer emission lines move CVs away from the colour locus of WDs, even if their continuum flux is dominated by the WD. No CV is located in the A-star exclusion box, and the WDMS binary exclusion box contains SDSSJ 0751+1444 (PQ Gem), SDSSJ 0808+3131, SDSSJ 0900+4301, SDSSJ 0938+0714 (PG 0935+075), and SDSSJ 1554+2721. All five systems have $P_{\rm orb} > 150$ min, and are hence not included in the discussion in Sections 3 and 4. Their location in the WDMS exclusion box is explained by the strong contribution of their companion stars (or, in the case of PQ Gem, a field M-dwarf included in the SDSS fibre). It may hence be that long-period CVs with low-accretion rates (i.e. visible companion star) may be under-represented in the SDSS CV sample. We conclude that the exclusion boxes in the SDSS quasar follow-up have no noticeable effect on the conclusions drawn here.
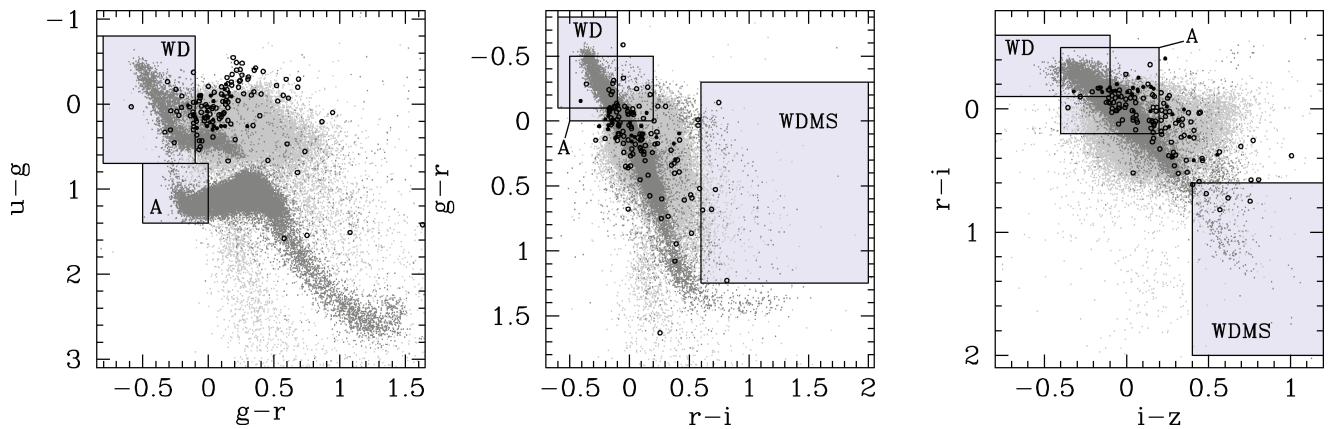
Figure 6. WD, A-star and WDMS binary *ugriz* exclusion boxes in the spectroscopic follow-up of SDSS quasar candidates. To be excluded from spectroscopic follow-up, an object must be located in all three (WD, A-star) or two (WDMS) boxes. The distribution of stars is shown by dark grey dots, that of quasars by light grey dots. The SDSS CVs from Tables 1 and 2 are shown in black, with the filled circles representing the WD-dominated CVs.

5.2.2 Bias in the follow-up strategy

An obvious question is *have we biased our follow-up in a way that would favour observations of short-period CVs*? If such a bias existed, the orbital period distribution resulting from the follow-up work would be skewed even within the SDSS CV sample, independent of the question of how representative this sample is of the true Galactic CV population. As shown in Section 4, a large fraction of the systems in the period spike have WD-dominated optical spectra. Among the remaining ∼130 SDSS CVs with no accurate period determination, the fraction of WD-dominated systems is similar to that within the sample of well-studied systems discussed here, suggesting that the period distribution of these remaining systems should be overall similar to the one shown here. In addition, at least the earlier follow-up studies of SDSS CVs focused on brighter systems, for the obvious reason of them being easier observational targets. Hence, the early follow-up was more likely to target intrinsically bright systems, which implies relatively high accretion rates, and on average periods above the spike. Finally, as it is evident from Fig. 2 (right-hand panel), the 45 previously known CVs with accurate periods *do not* show a period minimum spike. Among the ∼130 SDSS CVs with no accurate period, there is only a handful of additional previously known systems, and one might expect that the fraction of systems within the period spike will be higher in the remaining new SDSS discoveries. In summary, we are confident that our follow-up strategy has not introduced a significant bias with respect to the orbital periods of the systems studied so far. However, given that the fraction of well-studied systems among the SDSS CV sample is still relatively small (<50 per cent), further follow-up work is highly desirable to improve the statistics of the results presented here.

5.2.3 Magnetic CVs

Another caveat to bear in mind is that the intrinsic and observed CV populations may be made up of different evolutionary channels. It has been suggested that the strong magnetic field in polars will reduce the rate at which magnetic braking extracts angular orbital momentum (Webbink & Wickramasinghe 2002), which would result in different evolutionary time-scales (and hence different period distributions) between non-magnetic and strongly magnetic CVs. In the standard scenario of CV evolution, magnetic braking ceases at $P_{\mathrm{orb}} \simeq 3$ h, and hence the populations of polars and non-magnetic

CVs should differ most dramatically above the period gap. Plus, as polars do not suffer a discontinuous change in angular momentum loss, they are not expected to exhibit a period gap. One piece of observational evidence supporting the hypothesis that polars above the period gap have lower mass transfer rates, and hence are likely subject to lower rates of angular momentum loss, is that the WDs in polars have consistently lower effective temperatures than those in non-magnetic CVs (Sion 1991; Townsley & Bildsten 2003; Araujo-Betancor et al. 2005a). A similar behaviour is observed below the period gap, though at a much lower level (Araujo-Betancor et al. 2005a), which may suggest that non-magnetic CVs below the period gap are subject to some amount of residual magnetic braking, causing slightly higher mass transfer rates than found in short-period polars. Such differences in angular momentum loss rates should result in different orbital minimum periods for polars and non-magnetic CVs – which is, however, not observed. For completeness, we show in Fig. 7 the binned and cumulative period distributions of polars in the SDSS CVs and the non-SDSS CV samples. The fraction of polars in the SDSS CV sample is ∼20 per cent, compatible with the fraction among all known CVs (Wickramasinghe & Ferrario 2000).

Formally, a KS test on the cumulative period distributions of the non-magnetic SDSS CVs and the SDSS polars results in a 3.2 per cent probability for both sets being drawn from the same parent sample, which seems to suggest an intrinsic difference between these two samples. Comparing the polars among the non-SDSS CVs and the SDSS polars, the probability that both sets are drawn from the same parent population is 27 per cent, i.e. the two samples are broadly consistent in their period distribution. Taking these numbers at face value, the SDSS polars appear to have a different period distribution from the non-magnetic SDSS CVs. Eye-balling the distributions in Fig. 7, the accumulation of SDSS polars around 114 min is striking, and is in fact the dominant culprit for the statistical differences between the three CV samples inspected here. Tables 1 and 2 reveal that this accumulation is predominantly made up of the previously known systems, which were all identified as CVs because of their X-ray emission. The significance of this '114 min spike' has been debated when a total of only 15 polars were known, and has been suggested to be related to the resumption of mass transfer at the lower end of the period gap (Hameury, King & Lasota 1990). In the period distribution of all >80 polars, selected in the vast majority of cases from X-ray surveys, this spike is gone. We conclude that this feature, when identified 20 years ago, served
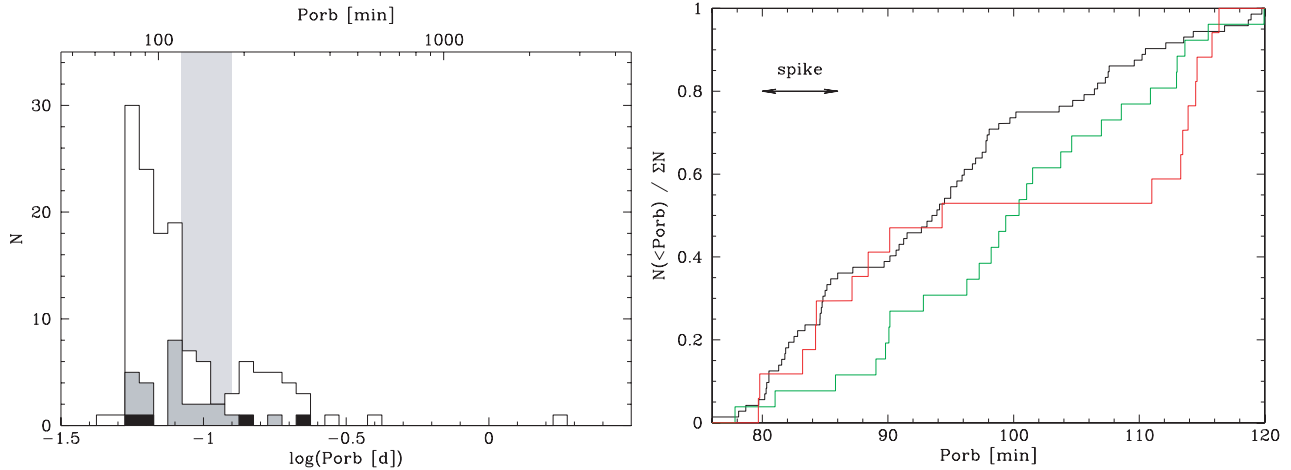
Figure 7. Left-hand panel: the orbital period distributions of non-magnetic SDSS CVs (Tables 1 and 2, white histograms), the 25 polars among the SDSS CVs (grey) and the four IPs among the SDSS CVs (black). Right-hand panel: cumulative period distributions of the SDSS CVs (short dashed), the 17 polars among the SDSS CVs with $P_{orb} \leq 120$ min (dotted) and 54 polars among the non-SDSS CVs (solid). The distribution of the polars among the SDSS CVs features an accumulation of systems around 114 min, which is predominantly made up of previously known systems. This 'spike' has been suggested to be the signature of the resumption of mass transfer at the lower edge of the period gap (Hameury et al. 1990), but this interpretation is doubtful in light of the much more detailed period distribution of polars available today.

as a powerful demonstration of small number statistics, and fulfils the same job a second time around, as it happens that most of the long-known '114 min' polars are in the SDSS footprint, whereas many of the polars found since then, e.g. in the RASS, are not.

5.2.4 Thermal time-scale mass transfer CVs

Another channel that is likely to add noticeably to the CV population are systems which started with a mass ratio $M_{donor}/M_{WD} \gtrsim 1$, and underwent a phase of thermal time-scale mass transfer (TTMT) before evolving into CVs (Schenker et al. 2002; Podsiadlowski, Han & Rappaport 2003; Kolb & Willems 2005). A number of suspected post-TTMT systems have been found (e.g. Thorstensen et al. 2002a,b; Gänsicke et al. 2003), but again their number is too small to assess their effect on the overall orbital period distribution of CVs.

5.3 Implications on cataclysmic variable population models

From our follow-up studies of CVs discovered by SDSS we have identified the 'spike' at the minimum period predicted by theory for two decades. Bearing in mind the caveats outlined above, what other implications can we derive from the SDSS CV sample at the current stage of follow-up, with only about half of the systems having reliable orbital periods?

5.3.1 Angular momentum loss rates below the period gap

Standard population models with gravitational wave radiation as the only driver of mass transfer in CVs below the period gap place the period minimum spike near 70 min (Kolb & Baraffe 1999; Barker & Kolb 2003). Tidal and rotational corrections of the underlying one-dimensional stellar models do not affect the position of the systems' period bounce, a finding supported by a three-dimensional SPH model of Roche-lobe filling stars (Renvoizé et al. 2002). Our discovery of a period spike near 80 min strongly favours the view that the observed CV period minimum is indeed the result of a

period bounce at 80 min, and that the theoretically calculated period minimum is too short by about 10 min.

The observed and calculated period minimum can be reconciled if either the orbital braking is about four times the value provided by gravitational wave radiation (Kolb & Baraffe 1999), or if the theoretical models underestimate the stellar radius for a given mass by about 20 per cent (Barker & Kolb 2003). An immediate consequence of the former interpretation is that the fraction of systems below the period gap, the fraction of post-period bounce systems, and the space density of CVs should be smaller than in the canonical model by, for example, Kolb (1993).

The absence of a period minimum spike plagued theorists working on compact binary evolution for more than two decades. King et al. (2002) showed that it is possible to obtain a more or less flat period distribution from subpopulations with different AM loss rates, up to five times the rate of gravitational wave radiation and fine-tuned contributions to the full population. Here, we have shown that a period minimum spike exists. Fig. 3 suggests that the spike is limited by two breaks in the slope of the cumulative period distribution, located at 80 min and 86 min, defining an approximate width of $\simeq 6$ min. The period spike can be fit with a binned Gaussian model. We used a Monte Carlo simulation assuming a Gaussian distribution to estimate 1σ errors on the parameters. This exercise results in the period of the spike, $P_{spike} = 82.4 \pm 0.7$ min and its width FWHM $_{spike} = 5.7 \pm 1.7$ min. We stress that these values are only valid under the assumption of a Gaussian distribution, but do illustrate that a more detailed assessment of the spike structure will require a larger set of periods accurate to better than 1 min. The sharp minimum period, coupled with the finite width of the spike, strongly suggests that for the bulk of CVs below the period gap there is very little variation in the secular mean value of the AM loss rate for systems with similar parameters. The width of the observed spike appears slightly larger than typically predicted by population models (~ 1.5–3 min), however given that we requested for all CVs in the sample discussed in this paper $\sigma(P_{orb})/P_{orb} \leq 3$ per cent, the intrinsic width of the period spike is not properly resolved, underlining the need for accurate period measurements.

5.3.2 The scaleheight of cataclysmic variables

A simple statement on the scaleheight of CVs can be made simply from comparing the SDSS subsamples for $g_{lim} = 19.0$, i.e. the CVs from the main quasar sample (which we have assumed to be approximately complete due to the colour overlap between CVs and quasars), and the full sample with $g_{lim} = 22.5$ (where SDSS makes no attempt to achieve any level of completeness, but merely allocates spare fibres to faint quasar candidates). A simple scaling of the survey volumes predicts an increase in the number of CVs by $\sim$1.4 for an assumed $H_z = 190$ pc. This modest gain comes from the fact that, with a limiting distance of 302 pc, the main quasar survey at $g_{lim} = 19.0$ already extends out to $\sim$1.6 scaleheights, and not many more CVs are found by going further into the halo. However, for an assumed $H_z = 260$ pc, the increase in the number of CVs found by going to g_{lim} is expected to be $\sim$4. Going to $g_{lim} = 22.5$ boosts the number of CVs actually found by SDSS by $\sim$1.5, which exceeds the prediction for $H_z = 190$ pc. This is a very conservative lower limit, as (a) the spectroscopic follow-up of faint quasar candidates is very incomplete down to $g_{lim} = 22.5$ (Richards et al. 2004), and (b) there are 16 more published WD-dominated systems without orbital period determinations, of which 14 have $g > 19.0$. Given the properties of the systems shown in Fig. 4, there is a $\sim$80 per cent probability that those 16 systems will have periods $P_{orb} \leq 86$ min as well. We conclude from this empirical study that the scaleheight of CVs is very likely larger than the 190 pc used by Patterson (1984), in agreement with the arguments of Pretorius et al. (2007) and the study by van Paradijs et al. (1996).

5.3.3 The space density of 'WZ Sge' stars

Assuming the standard CV evolution theory, and a mid-plane CV space density of 5×10^{-5} pc^{-3}, Pretorius et al. (2007) calculated the period distributions of various magnitude-limited samples, and found that the period minimum spike decreases in prominence for brighter magnitude limits, although it was still present in a sample with $V < 14$ with a contrast of two with respect to neighbouring periods .

In Fig. 8, we show the period distributions of the SDSS CVs, as before divided in new and old systems, for the four different magnitude limits used in the previous sections, $g_{lim} = 22.5$, 19.0, 17.4, 16.1. The accumulation of systems at the minimum period is clearly present in the full sample, and still so once a $g_{lim} = 19.0$ cut is applied. At $g_{lim} = 17.4$, the number of systems in the shortest-period bin still exceeds all other three bins below the period gap, but the numbers are too small to draw any firm conclusion. This being said, we note that a similar 'accumulation' in the shortest-period bin was found in the period distribution of HQS CVs, which is an independent sample with the same magnitude limit (see fig. 18 of Aungwerojwit et al. 2006). Cutting to $g_{lim} = 16.1$, the limit of the PG Survey, only five systems are left below the period gap, and hence no statement with regard to a period spike can be done.

From Fig. 8, it is clear that SDSS is picking up many CVs with $P_{orb} \leq 120$ min at magnitudes fainter than $g_{lim} \simeq 17.4$. In particular, SDSS has found a large number of CVs that have WD-dominated optical spectra, which must have very low mass donor stars as little or no spectral features from the companions are seen, and orbital periods right at the minimum period. Taking their properties at face value, it appears likely that all these systems are WZ Sge type dwarf novae, with very long outburst recurrence times. There is no plausible selection mechanism within the fibre allocation of SDSS that would go *against* finding this type of system at bright magni-
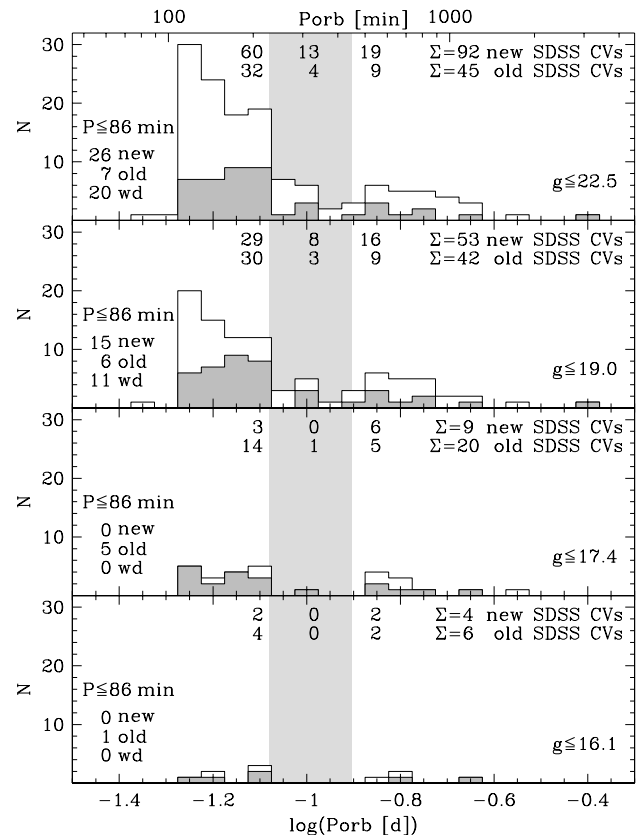

Figure 8. The orbital period distributions of the new SDSS CVs (Table 1, white histograms) and the old SDSS CVs (Table 2, grey) applying four different magnitude limits. From top to bottom: $g \leq 22.5$, corresponding to the faintest CV included in our sample; $g \leq 19.0$, corresponding to the magnitude limit of the low-redshift quasar survey within SDSS; $g \leq 17.5$, corresponding to the magnitude limit of the HQS; and $g \leq 16.1$, corresponding to the magnitude limit of the PG Survey. The number of systems below, in and above the 2–3 h period gap as well as their sum are given in each panel, with the values for the new SDSS CVs being on top of those for the old SDSS CVs. The number of new SDSS CVs, old SDSS CVs and WD-dominated CVs in the $\sim$80–86 min period spike are shown on the left-hand side of the period histogram.

tudes $g \simeq 15$–17.4, but not a single bright WZ Sge candidate has been found by SDSS (the brightest one being SDSSJ 1339+4847, $g = 17.6$). Fig. 9 compares the magnitude distributions of non-magnetic SDSS CVs with a WD-dominated spectrum and of those in which the WD is not visible. Both distributions peak at $g \simeq 19$, i.e. the magnitude limit of the main quasar sample, implying that the completeness of the SDSS CV sample drops substantially at $g \geq 19$. The WD-dominated systems ramp up in numbers only at faint magnitudes corresponding to distances $d \gtrsim 150$ pc, suggesting that they are intrinsically relatively rare.

This suggestion is confirmed by looking at how many bright WZ Sge (candidate) stars were known prior to SDSS. In Table 4, we list the WZ Sge (candidate) systems from Ritter & Kolb (2003) (V7.9) which are brighter than $V \simeq 17$ in quiescence. The absolute magnitudes for these five systems, $\langle M_V \rangle = 11.6 \pm 0.5$, agree well with our estimate for the WD-dominated SDSS systems (Section 5.1.1). WZ Sge and GW Lib were discovered through their large-amplitude outbursts, BW Scl, GD 552 and V455 And were identified through follow-up spectroscopy of *ROSAT* X-ray sources, high proper motion objects, and emission line stars from the HQS, respectively. With the exception of GD 552, all systems
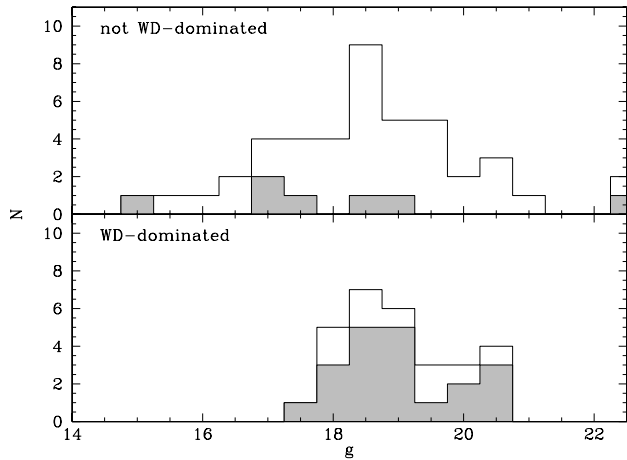
Figure 9. Top panel: *g*-band magnitude distribution of non-magnetic SDSS CVs which do not exhibit broad photospheric WD Balmer absorption lines in their optical spectra. Shown in white are all systems with $P_{orb} < 120$ min, i.e. below the period gap. Systems within the 'period minimum spike', $P_{orb} \leq 86$ min are shown in grey. Bottom panel: same as above, but for the WD-dominated SDSS CVs ('WZ Sge candidates').

Table 4. WZ Sge candidate systems brighter than $V \simeq 17$ identified prior to SDSS.

System	V_q	$d(pc)$	M_V	Ref.
WZ Sge	15.0	$43 \pm {}^{1.6}_{1.5}$	11.8	1,2,3
BW Scl	16.4	131 ± 18	10.8	4,5,6
GD 552	16.5	105 ± 20	11.4	7,8
V455 And	16.5	$74 \pm {}^{8}_{7}$	12.2	9,10
GW Lib	16.7	$104 \pm {}^{30}_{20}$	11.6	2,11

[1]Mackie (1920), [2]Thorstensen (2003), [3]Harrison et al. (2004), [4]Augusteijn & Wisotzki (1997), [5]Abbott, Fleming & Pasquini (1997), [6]Gänsicke et al. (2005), [7]Greenstein & Giclas (1978), [8]Unda-Sanzana et al. (2008), [9]Araujo-Betancor et al. (2005b), [10]Gänsicke et al. (in preparation), [11]González (1983).

have WD-dominated spectra with no spectroscopic evidence for the mass donors. Thus, it appears that no matter what selection method is used, WZ Sge stars are not very numerous.

The standard CV population models predict that $\sim$99 per cent of all CVs should have periods $\lesssim 2$ h, and $\sim$70 per cent should be post-bounce systems (Kolb 1993; Howell et al. 2001). If we follow Pretorius et al. (2007), and take the average of the space densities predicted by CV evolution theory, $\rho = 5 \times 10^{-5}$ pc^{-3} (de Kool 1992; Politano 1996), we expect $\sim$210 CVs within a radius of 100 pc of the Earth, and practically all of them should be short-period systems, of which $\sim$150 post-bounce. If the CV space density were as high as theory predicts, comparing the numbers discussed above implies (a) the bulk of CVs has still not been found, and (b) the majority of period bouncers must differ in terms of their colours and spectra from the typical 'WZ Sge' stars.

6 CONCLUSIONS

SDSS is providing us with the largest, deepest and most homogeneously selected CV sample so far, and holds the potential of detailed tests of the current models of compact binary evolution. Follow-up studies are currently available for about half of the SDSS CVs, and we have analysed the global properties of this sample,

with particular emphasis on the numerous short-period systems. In summary, we find as follows.

(i) The period distribution of the SDSS CVs differs significantly from that of any previous CV sample, containing a much larger fraction of short-period CVs. Most striking is the appearance of an accumulation of CVs with $80 \lesssim P_{orb} \lesssim 86$ min, which we identify as the period minimum spike predicted for two decades by CV population models. The finite width of the spike suggests that the angular momentum loss rates below the period gap must fall into a narrow range.

(ii) Within the period minimum spike, the majority of new CVs identified by SDSS differ substantially from the bulk of the previously known short-period CVs. Their optical spectra are dominated by the WD, with no discernable signature from the mass donors, and only a few of them have so far exhibited 'typical' CV accretion activity, i.e. X-ray emission or dwarf nova outbursts. We determine an average absolute magnitude of $\langle M_g \rangle = 11.6 \pm 0.7$ for these systems. The spectra are usually devoid of spectroscopic signatures from the mass donors, implying very late spectral types and low masses. Work by Littlefair et al. (2006b, 2007, 2008) confirms that a high fraction of the eclipsing systems in the period minimum spike contain brown dwarf donors.

(iii) Comparison with the HQS and the PG Survey suggests that the main advantage of SDSS is indeed its unprecedented depth. Comparing subsamples of the SDSS CVs with different magnitude limits indicates that the scaleheight of short-period CVs is $H_z > 190$ pc.

(iv) While WZ Sge stars are often considered to be period bounce candidate, the number of WZ Sge stars found so far is too small to account for the space density of post-bounce systems predicted by population models.

(v) Accurate period determinations should be obtained for the remaining $\sim$130 SDSS CVs, which will not only allow to put the results presented here on a more robust statistical base, but also to carry out more detailed investigations into the shape and width of the period minimum spike, and to address questions such as whether strongly magnetic CVs evolve differently from non-magnetic systems.

NOTE ADDED IN PROOF

We note that the periods calculated from Eq. (1) differ by less than 1% from those obtained with the relation by Stolz & Schoembs (1984), which is a remarkable agreement given the small number of systems used in the original calibration of this method. Official GCVS names have been allocated to the following new SDSS CVs:

SDSSJ 015543.40+002807.2 = FL Cet,
SDSSJ 155331.11+551614.4 = MQ Dra,
SDSSJ 132411.57+032050.4 = PZ Vir,
SDSSJ 161033.63−010223.3 = V386 Ser.

We thank Hans Ritter for bringing this to our attention.

been an important resource of information for the research presented here. Funding for the SDSS has been provided by the Alfred P. Sloan Foundation, the Participating Institutions, the National Aeronautics and Space Administration, the National Science Foundation, the US Department of Energy, the Japanese Monbukagakusho and the Max Planck Society. The SDSS website is http://www.sdss.org. We would like to thank the amateur community worldwide for their dedicated monitoring of the SDSS CVs. Finally, we thank Joe Patterson for a constructive referee report.

REFERENCES

Abbott T. M. C., Fleming T. A., Pasquini L., 1997, A&A, 318, 134
Adelman-McCarthy J. K. et al., 2007, ApJS, 172, 634
Ak T., Retter A., Liu A., Esenoğlu H. H., 2005, Publ. Astron. Soc. Aust., 22, 105
Ak T., Bilir S., Ak S., Eker Z., 2008, New Astron., 13, 133
Araujo-Betancor S., Gänsicke B. T., Long K. S., Beuermann K., de Martino D., Sion E. M., Szkody P., 2005a, ApJ, 622, 589
Araujo-Betancor S. et al., 2005b, A&A, 430, 629
Arras P., Townsley D. M., Bildsten L., 2006, ApJ, 643, L119
Augusteijn T., Wisotzki L., 1997, A&A, 324, L57
Aungwerojwit A. et al., 2005, A&A, 443, 995
Aungwerojwit A. et al., 2006, A&A, 455, 659
Barker J., Kolb U., 2003, MNRAS, 340, 623
Berg C., Wegner G., Foltz C. B., Chaffee F. H., J., Hewett P. C., 1992, ApJS, 78, 409
Berger E. et al., 2005, Nat, 438, 988
Bergeron P., Wesemael F., Beauchamp A., 1995, PASP, 107, 1047
Bond H. E., White R. L., Becker R. H., O'Brien M. S., 2002, PASP, 114, 1359
Bonnet-Bidaud J. M., Mouchet M., Somova T. A., Somov N. N., 1996, A&A, 306, 199
Boyd D., Oksanen A., Henden A., 2006, J. Br. Astron. Assoc., 116, 187
Boyd D., Shears J., Koff R., 2008, J. Br. Astron. Assoc., 118, 199
Burleigh M. R. et al., 2006, MNRAS, 373, 1416
Burwitz V. et al., 1998, A&A, 331, 262
Casares J., Charles P. A., Naylor T., 1992, Nat, 355, 614
Copperwheat C. M. et al., 2009, MNRAS, 393, 157
Cropper M., 1989, MNRAS, 236, 935
de Kool M., 1992, A&A, 261, 188
Dhillon V. S., Jones D. H. P., Marsh T. R., Smith R. C., 1992, MNRAS, 258, 225
Dillon M. et al., 2008, MNRAS, 386, 1568
Drake A. J. et al., 2009, ApJ, 696, 870
Farihi J., Burleigh M. R., Hoard D. W., 2008, ApJ, 674, 421
Faulkner J., 1971, ApJ, 170, L99
Feline W. J., Dhillon V. S., Marsh T. R., Brinkworth C. S., 2004a, MNRAS, 355, 1
Feline W. J., Dhillon V. S., Marsh T. R., Stevenson M. J., Watson C. A., Brinkworth C. S., 2004b, MNRAS, 347, 1173
Feline W. J., Dhillon V. S., Marsh T. R., Watson C. A., Littlefair S. P., 2005, MNRAS, 364, 1158
Gänsicke B. T., 2005, in Hameury J.-M., Lasota J.-P., eds, ASP Conf. Ser. Vol. 330, The Astrophysics of Cataclysmic Variables and Related Objects. Astron. Soc. Pac., San Francisco, p. 3
Gänsicke B. T., Sion E. M., Beuermann K., Fabian D., Cheng F. H., Krautter J., 1999, A&A, 347, 178
Gänsicke B. T., Fried R. E., Hagen H.-J., Beuermann K., Engels D., Hessman F. V., Nogami D., Reinsch K., 2000, A&A, 356, L79
Gänsicke B. T., Hagen H. J., Engels D., 2002, in Gänsicke B. T., Beuermann K., Reinsch K., eds, ASP Conf. Ser. Vol. 261, The Physics of Cataclysmic Variables and Related Objects. Astron. Soc. Pac., San Francisco, p. 190
Gänsicke B. T. et al., 2003, ApJ, 594, 443
Gänsicke B. T., Szkody P., Howell S. B., Sion E. M., 2005, ApJ, 629, 451
Gänsicke B. T. et al., 2006, MNRAS, 365, 969

Gehrels N. et al., 2005, Nat, 437, 851
Gianninas A., Bergeron P., Fontaine G., 2006, AJ, 132, 831
González L. E., 1983, IAU Circ., 3854
Green R. F., Ferguson D. H., Liebert J., Schmidt M., 1982, PASP, 94, 560
Green R. F., Schmidt M., Liebert J., 1986, ApJS, 61, 305
Greenstein J. L., Giclas H., 1978, PASP, 90, 460
Hameury J. M., King A. R., Lasota J. P., 1990, MNRAS, 242, 141
Harrison T. E., Johnson J. J., McArthur B. E., Benedict G. F., Szkody P., Howell S. B., Gelino D. M., 2004, AJ, 127, 460
Hellier C., Ramseyer T. F., Jablonski F. J., 1994, MNRAS, 271, L25
Hoard D. W., Szkody P., 1997, ApJ, 481, 433
Hoard D. W., Linnell A. P., Szkody P., Fried R. E., Sion E. M., Hubeny I., Wolfe M. A., 2004, ApJ, 604, 346
Homer L. et al., 2005, ApJ, 620, 929
Homer L., Szkody P., Chen B., Henden A., Schmidt G., Anderson S. F., Silvestri N. M., Brinkmann J., 2006a, AJ, 131, 562
Homer L., Szkody P., Henden A., Chen B., Schmidt G. D., Fraser O. J., West A. A., 2006b, AJ, 132, 2743
Horne K., Marsh T. R., Cheng F. H., Hubeny I., Lanz T., 1994, ApJ, 426, 294
Howell S., Szkody P., 1988, PASP, 100, 224
Howell S. B., Warnock A., Mason K. O., Reichert G. A., Kreidl T. J., 1988, MNRAS, 233, 79
Howell S. B., Szkody P., Kreidl T. J., Mason K. O., Puchnarewicz E. M., 1990, PASP, 102, 758
Howell S. B., Sirk M. M., Malina R. F., Mittaz J. P. D., Mason K. O., 1995a, ApJ, 439, 991
Howell S. B., Szkody P., Cannizzo J. K., 1995b, ApJ, 439, 337
Howell S. B., Rappaport S., Politano M., 1997, MNRAS, 287, 929
Howell S. B., Nelson L. A., Rappaport S., 2001, ApJ, 550, 897
Jester S. et al., 2005, AJ, 130, 873
Jiang X. J., Engels D., Wei J. Y., Tesch F., Hu J. Y., 2000, A&A, 362, 263
Justham S., Rappaport S., Podsiadlowski P., 2006, MNRAS, 366, 1415
Kalogera V., Kolb U., King A. R., 1998, ApJ, 504, 967
Katajainen S., Lehto H. J., Piirola V., Karttunen H., Piironen J., 2000, A&A, 357, 677
Kato T., Kiyota S., Novak R., Matsumoto K., 1999, Inf. Bull. Var. Stars, 4794, 1
Kato T., Nogami D., Matsumoto K., Baba H., 2004, PASJ, 56, 109
Kato T. et al., 2009, PASJ, in press (arXiv:0905.1757)
King A. R., Schenker K., Hameury J. M., 2002, MNRAS, 335, 513
Knigge C., 2006, MNRAS, 373, 484
Knigge C., Long K. S., Hoard D. W., Szkody P., Dhillon V. S., 2000, ApJ, 539, L49
Kolb U., 1993, A&A, 271, 149
Kolb U., Baraffe I., 1999, MNRAS, 309, 1034
Kolb U., Willems B., 2005, in Hameury J.-M., Lasota J.-P., eds, ASP Conf. Ser. Vol. 330, The Astrophysics of Cataclysmic Variables and Related Objects. Astron. Soc. Pac., San Francisco, p. 17
Liebert J., Tapia S., Bond H. E., Grauer A. D., 1982, ApJ, 254, 232
Littlefair S. P., Dhillon V. S., Marsh T. R., Gänsicke B. T., 2006a, MNRAS, 371, 1435
Littlefair S. P., Dhillon V. S., Marsh T. R., Gänsicke B. T., Southworth J., Watson C. A., 2006b, Science, 314, 1578
Littlefair S. P., Dhillon V. S., Marsh T. R., Gänsicke B. T., Baraffe I., Watson C. A., 2007, MNRAS, 381, 827
Littlefair S. P., Dhillon V. S., Marsh T. R., Gänsicke B. T., Southworth J., Baraffe I., Watson C. A., Copperwheat C., 2008, MNRAS, 388, 1582
Mackie J., 1920, Astron. Nachr., 210, 79
Martinez-Pais I. G., Casares J., 1995, MNRAS, 275, 699
Mennickent R. E., Tovmassian G., Zharikov S. V., Tappert C., Greiner J., Gänsicke B. T., Fried R. E., 2002, A&A, 383, 933
Misselt K. A., Shafter A. W., 1995, AJ, 109, 1757
Morris S. L., Schmidt G. D., Liebert J., Stocke J., Gioia I. M., Maccacaro T., 1987, ApJ, 314, 641
Mukadam A. S., Winget D. E., von Hippel T., Montgomery M. H., Kepler S. O., Costa A. F. M., 2004, ApJ, 612, 1052

Mukadam A. S., Gänsicke B. T., Szkody P., Aungwerojwit A., Howell S. B., Fraser O. J., Silvestri N. M., 2007, ApJ, 667, 433

Nelemans G., Tout C. A., 2005, MNRAS, 356, 753

Nilsson R., Uthas H., Ytre-Eide M., Solheim J.-E., Warner B., 2006, MNRAS, 370, L56

Nogami D., Kato T., Masuda S., Hirata R., Matsumoto K., Tanabe K., Yokoo T., 1995, PASJ, 47, 897

Nogami D., Kato T., Hirata R., 1996, PASJ, 48, 607

Nogami D., Masuda S., Kato T., 1997, PASP, 109, 1114

Nogami D., Kato T., Baba H., Masuda S., 1998, PASJ, 50, L1

Nogami D., Engels D., Gänsicke B. T., Pavlenko E. P., Novák R., Reinsch K., 2000, A&A, 364, 701

O'Donoghue D. et al., 2006, MNRAS, 372, 151

Osaki Y., 1995a, PASJ, 47, L11

Osaki Y., 1995b, PASJ, 47, L25

Osborne J. P., Beardmore A. P., Wheatley P. J., Hakala P., Watson M. G., Mason K. O., Hassall B. J. M., King A. R., 1994, MNRAS, 270, 650

Paczynski B., 1986, ApJ, 308, L43

Paczynski B., Sienkiewicz R., 1981, ApJ, 248, L27

Paczyński B., Sienkiewicz R., 1983, ApJ, 268, 825

Patterson J., 1984, ApJS, 54, 443

Patterson J., 1998, PASP, 110, 1132

Patterson J. et al., 1998, PASP, 110, 1290

Patterson J., Kemp J., Jensen L., Vanmunster T., Skillman D. R., Martin B., Fried R., Thorstensen J. R., 2000a, PASP, 112, 1567

Patterson J. et al., 2000b, PASP, 112, 1584

Patterson J. et al., 2003, PASP, 115, 1308

Patterson J. et al., 2004, PASP, 116, 516

Patterson J. et al., 2005, PASP, 117, 1204

Patterson J., Thorstensen J. R., Knigge C., 2008, PASP, 120, 510

Pavlenko E. et al., 2007, in Napiwotzki R., Burleigh R., eds, ASP Conf. Ser. Vol. 372, 15th European Workshop on White Dwarfs. Astron. Soc. Pac., San Francisco, p. 511

Peters C. S., Thorstensen J. R., 2005, PASP, 117, 1386

Podsiadlowski P., Han Z., Rappaport S., 2003, MNRAS, 340, 1214

Politano M., 1996, ApJ, 465, 338

Potter S. B., O'Donoghue D., Romero-Colmenero E., Buckley D. A. H., Woudt P. A., Warner B., 2006, MNRAS, 371, 727

Pretorius M. L., Woudt P. A., Warner B., Bolt G., Patterson J., Armstrong E., 2004, MNRAS, 352, 1056

Pretorius M. L., Knigge C., Kolb U., 2007, MNRAS, 374, 1495

Rappaport S., Joss P. C., Webbink R. F., 1982, ApJ, 254, 616

Rappaport S., Joss P. C., Verbunt F., 1983, ApJ, 275, 713

Remillard R. A., Schachter J. F., Silber A. D., Slane P., 1994, ApJ, 426, 288

Renvoizé V., Baraffe I., Kolb U., Ritter H., 2002, A&A, 389, 485

Richards G. T. et al., 2002, AJ, 123, 2945

Richards G. T. et al., 2004, ApJS, 155, 257

Ringwald F., 1993, PhD thesis, Dartmouth College

Ringwald F. A., Thorstensen J. R., Hamwey R. M., 1994, MNRAS, 271, 323

Ritter H., Kolb U., 2003, A&A, 404, 301

Robertson J. W., Honeycutt R. K., Turner G. W., 1995, PASP, 107, 443

Rodrigues C. V., Jablonski F. J., D'Amico F., Cieslinski D., Steiner J. E., Diaz M. P., Hickel G. R., 2006, MNRAS, 369, 1972

Rodríguez-Gil P., Gänsicke B. T., Araujo-Betancor S., Casares J., 2004, MNRAS, 349, 367

Rodríguez-Gil P., Schmidtobreick L., Gänsicke B. T., 2007a, MNRAS, 374, 1359

Rodríguez-Gil P. et al., 2007b, MNRAS, 377, 1747

Ruiz-Lapuente P. et al., 2004, Nat, 431, 1069

Schenker K., King A. R., Kolb U., Wynn G. A., Zhang Z., 2002, MNRAS, 337, 1105

Schmidt G. D., Hoard D. W., Szkody P., Melia F., Honeycutt R. K., Wagner R. M., 1999, ApJ, 525, 407

Schmidt G. D., Szkody P., Silvestri N. M., Cushing M. C., Liebert J., Smith P. S., 2005a, ApJ, 630, L173

Schmidt G. D. et al., 2005b, ApJ, 620, 422

Schmidt G. D., Szkody P., Henden A., Anderson S. F., Lamb D. Q., Margon B., Schneider D. P., 2007, ApJ, 654, 521

Schmidt G. D., Smith P. S., Szkody P., Anderson S. F., 2008, PASP, 120, 160

Schneider D. P. et al., 2007, AJ, 134, 102

Schwope A. D., Naundorf C. E., Thomas H.-C., Beuermann K., 1991, A&A, 244, 373

Schwope A. D., Brunner H., Buckley D., Greiner J., Heyden K. v. D., Neizvestny S., Potter S., Schwarz R., 2002, A&A, 396, 895

Shafter A. W., Szkody P., 1984, ApJ, 276, 305

Shafter A. W., Szkody P., Thorstensen J. R., 1986, ApJ, 308, 765

Shears J., Brady S., Foote J., Starkey D., Vanmunster T., 2008, J. Br. Astron. Assoc., 118, 288

Shears J., Klingenberg G., de Ponthiere P., 2007, J. Br. Astron. Assoc., 117, 331

Shears J., Brady S., Gänsicke B., Krajci T., Miller I., Ogmen Y., Pietz J., Staels B., 2009, J. Br. Astron. Assoc., 119, 114

Sion E. M., 1991, AJ, 102, 295

Skillman D. R., Patterson J., Thorstensen J. R., 1995, PASP, 107, 545

Southworth J., Gänsicke B. T., Marsh T. R., de Martino D., Hakala P., Littlefair S., Rodríguez-Gil P., Szkody P., 2006, MNRAS, 373, 687

Southworth J., Gänsicke B. T., Marsh T. R., de Martino D., Aungwerojwit A., 2007a, MNRAS, 378, 635

Southworth J., Marsh T. R., Gänsicke B. T., Aungwerojwit A., Hakala P., de Martino D., Lehto H., 2007b, MNRAS, 382, 1145

Southworth J., Townsley D. M., Gänsicke B. T., 2008a, MNRAS, 388, 709

Southworth J. et al., 2008b, MNRAS, 391, 591

Stanishev V., Kraicheva Z., Genkov V., 2006, A&A, 455, 223

Stark M. A., Wade R. A., Thorstensen J. R., Peters C. S., Smith H. A., Miller R. D., Green E. M., 2008, AJ, 135, 991

Steeghs D., Perryman M. A. C., Reynolds A., de Bruijne J. H. J., Marsh T., Dhillon V. S., Peacock A., 2003, MNRAS, 339, 810

Stolz B., Schoembs R., 1984, A&A, 132, 187

Szkody P., Gänsicke B. T., Howell S. B., Sion E. M., 2002a, ApJ, 575, L79

Szkody P., Gänsicke B. T., Sion E. M., Howell S. B., 2002b, ApJ, 574, 950

Szkody P. et al., 2002c, AJ, 123, 430

Szkody P. et al., 2003a, AJ, 126, 1499

Szkody P. et al., 2003b, ApJ, 583, 902

Szkody P. et al., 2004, AJ, 128, 1882

Szkody P. et al., 2005, AJ, 129, 2386

Szkody P. et al., 2006, AJ, 131, 973

Szkody P. et al., 2007a, AJ, 134, 185

Szkody P. et al., 2007b, ApJ, 658, 1188

Szkody P. et al., 2009, AJ, 137, 4011

Taylor C., 1999, PhD thesis, Dartmouth College

Thomas H. C., Beuermann K., 1998, Lecture Notes in Physics, Vol. 506, Springer Verlag, Berlin, p. 247

Thorstensen J. R., 1997, PASP, 109, 1241

Thorstensen J. R., 2003, AJ, 126, 3017

Thorstensen J. R., Armstrong E., 2005, AJ, 130, 759

Thorstensen J. R., Fenton W. H., 2002, PASP, 114, 74

Thorstensen J. R., Freed I. W., 1985, AJ, 90, 2082

Thorstensen J. R., Taylor C. J., 2001, MNRAS, 326, 1235

Thorstensen J. R., Smak J., Hessman F. V., 1985, PASP, 97, 437

Thorstensen J. R., Davis M. K., Ringwald F. A., 1991, AJ, 102, 683

Thorstensen J. R., Patterson J. O., Shambrook A., Thomas G., 1996, PASP, 108, 73

Thorstensen J. R., Fenton W. H., Patterson J., Kemp J., Halpern J., Baraffe I., 2002a, PASP, 114, 1117

Thorstensen J. R., Fenton W. H., Patterson J. O., Kemp J., Krajci T., Baraffe I., 2002b, ApJ, 567, L49

Thorstensen J. R., Patterson J., Kemp J., Vennes S., 2002c, PASP, 114, 1108

Thorstensen J. R., Fenton W. H., Taylor C. J., 2004, PASP, 116, 300

Tovmassian G. H., Greiner J., Zharikov S. V., Echevarría J., Kniazev A., 2001, A&A, 380, 504

Townsley D. M., Bildsten L., 2003, ApJ, 596, L227

Townsley D. M., Gänsicke B. T., 2009, ApJ, 693, 1007

Tramposch J., Homer L., Szkody P., Henden A., Silvestri N. M., Yirak K., Fraser O. J., Brinkmann J., 2005, PASP, 117, 262

Uemura M. et al., 2000, PASJ, 52, L9

Unda-Sanzana E. et al., 2008, MNRAS, 388, 889

van Paradijs J., Augusteijn T., Stehle R., 1996, A&A, 312, 93

Vanmunster T., Velthuis F., McCormick J., 2000, Inf. Bull. Var. Stars, 4955, 1

Verbunt F., Zwaan C., 1981, A&A, 100, L7

Voges W. et al., 2000, Int. Astron. Union Circ., 7432

Wagner R. M. et al., 1998, AJ, 115, 787

Warner B., 1986, MNRAS, 222, 11

Webbink R. F., Wickramasinghe D. T., 2002, MNRAS, 335, 1

Whelan J., Iben I. J., 1973, ApJ, 186, 1007

Wickramasinghe D. T., Ferrario L., 2000, PASP, 112, 873

Willems B., Kolb U., Sandquist E. L., Taam R. E., Dubus G., 2005, ApJ, 635, 1263

Wolfe M. A., Szkody P., Fraser O. J., Homer L., Skinner S., Silvestri N. M., 2003, PASP, 115, 1118

Woosley S. E., Taam R. E., Weaver T. A., 1986, ApJ, 301, 601

Woudt P. A., Warner B., 2004, MNRAS, 348, 599

Woudt P. A., Warner B., Pretorius M., 2004, MNRAS, 351, 1015

Woudt P. A., Warner B., Pretorius M. L., Dale D., 2005, in Hameury J.-M., Lasota J.-P., eds, ASP Conf. Ser. Vol. 330, The Astrophysics of Cataclysmic Variables and Related Objects. Astron. Soc. Pac., San Francisco, p. 325

Woudt P. A., Warner B., Pretorius M., 2009, MNRAS, submitted

York D. G. et al., 2000, AJ, 120, 1579

Zharikov S. V., Tovmassian G. H., Napiwotzki R., Michel R., Neustroev V., 2006, A&A, 449, 645

Zharikov S. V. et al., 2008, A&A, 486, 505

Zwitter T., Munari U., 1996, A&AS, 117, 449

This paper has been typeset from a TEX/LATEX file prepared by the author.